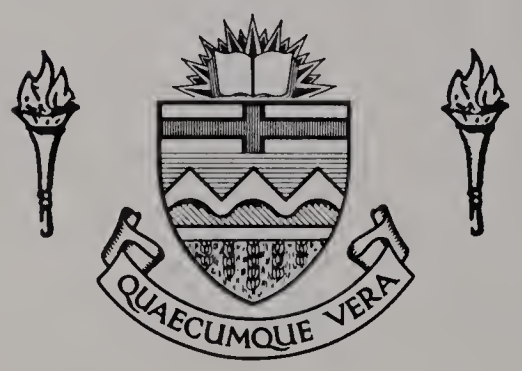
University of Alberta Library
0 1620 2191 8162

For Reference

NOT TO BE TAKEN FROM THIS ROOM

Ex libris
universitatis
albertaensis



THE UNIVERSITY OF ALBERTA

RELEASE FORM

NAME OF AUTHOR David W. Marshall

TITLE OF THESIS A COMPUTER MODEL TO DETERMINE THE TEMPERATURE DISTRIBUTION IN A WELLBORE

DEGREE FOR WHICH THESIS WAS PRESENTED MASTER OF SCIENCE

YEAR THIS DEGREE GRANTED SPRING, 1980

Permission is hereby granted to THE UNIVERSITY OF ALBERTA LIBRARY to reproduce single copies of this thesis and to lend or sell such copies for private, scholarly or scientific research purposes only.

The author reserves other publication rights, and neither the thesis nor extensive extracts from it may be printed or otherwise reproduced without the author's written permission.

THE UNIVERSITY OF ALBERTA

A COMPUTER MODEL TO DETERMINE THE TEMPERATURE DISTRIBUTION IN A WELLBORE

by

(C)

David W. Marshall

A THESIS

SUBMITTED TO THE FACULTY OF GRADUATE STUDIES AND RESEARCH

IN PARTIAL FULFILMENT OF THE REQUIREMENTS FOR THE DEGREE

OF MASTER OF SCIENCE

IN

PETROLEUM ENGINEERING

DEPARTMENT OF MINERAL ENGINEERING

EDMONTON, ALBERTA

SPRING, 1980

THE UNIVERSITY OF ALBERTA

FACULTY OF GRADUATE STUDIES AND RESEARCH

The undersigned certify that they have read, and recommend to the Faculty of Graduate Studies and Research, for acceptance, a thesis entitled A COMPUTER MODEL TO DETERMINE THE TEMPERATURE DISTRIBUTION IN A WELLBORE submitted by David W. Marshall in partial fulfilment of the requirements for the degree of MASTER OF SCIENCE in PETROLEUM ENGINEERING.

To

Mary and Claire

ABSTRACT

Previous methods of determining the wellbore temperature distribution have involved a compromise between accuracy, and the time required to obtain the information.

To overcome this problem, a computer model has been developed which utilizes a direct solution technique to solve the finite difference equations describing the transient heat transfer mechanisms in a wellbore during drilling operations. The method involves representing this system of equations by a heptadiagonal, asymmetric band matrix, and solving this matrix by means of a band algorithm.

A significant improvement in the solution time is achieved, thus allowing the model to be used at the wellsite to provide dynamic wellbore temperature distributions.

The results of a parametric sensitivity analysis carried out using the model indicate that a number of assumptions made in previous models are invalid, and that certain factors ignored in previous models, have a significant effect on the wellbore temperature distribution.

ACKNOWLEDGEMENTS

The author wishes to express his appreciation to Dr. R. G. Bentsen and Dr. S. M. Farouq Ali for their assistance throughout the course of this investigation.

Acknowledgement is also made to Dr. J. T. Ryan of the Department of Chemical Engineering and to the author's colleague, Mr. J. Blunschi for their valuable advice.

The author further wishes to thank the Petroleum Aid to Education for their financial support during the course of this study.

Thanks are also due to Mr. G. Bezaire of Esso Resources, Canada for providing useful information about current drilling practices in the area of research.

Table of Contents

Chapter Page

1. INTRODUCTION 1

2. REVIEW OF THE AVAILABLE MODELS 4

3. STATEMENT OF THE PROBLEM 7

4. THEORY AND DEVELOPMENT OF THE MODEL 8

4.1 Assumptions 10

4.2 Energy Balances 10

4.3 Solution of the Partial Differential Equations. ...12

4.4 The Selection of an Appropriate Rheological Model .19

4.5 Non-Newtonian Convective Heat Transfer Coefficients 27

4.6 Calculation of the Energy Source Terms 33

4.6.1 Drill String 36

4.6.2 Drill Bit 41

4.6.3 Annulus 42

5. DISCUSSION OF RESULTS 47

5.1 Comparison with Previous Models 47

5.2 Parametric Sensitivity Analysis 52

5.3 Validity of the Assumptions 69

5.4 Wellsite Operation of the Model 70

6. SUMMARY AND CONCLUSIONS 73

6.1 Suggestions for Further Research 74

REFERENCES 76

APPENDIX I - DERIVATION OF THE PARTIAL DIFFERENTIAL EQUATIONS DESCRIBING THE TRANSIENT HEAT FLOW IN A WELLBORE 80

APPENDIX II - DERIVATION OF THE FINITE DIFFERENCE EQUATIONS 85

APPENDIX III - SUBROUTINE LEQT1B 90

List of Tables

Table		Page
4.1	Reference data for the wellbore thermal model ...	21
4.2	Comparison of non-Newtonian convective heat transfer coefficients for turbulent pipe flow of power law fluids	29
4.3	Comparison of non-Newtonian convective heat transfer coefficients for laminar annular flow of power law fluids. (Inner and outer walls respectively)	30
4.4	Comparison of non-Newtonian Nusselt numbers for laminar pipe flow of power law fluids	31
4.5	Comparison of Fanning friction factor equations for turbulent flow in smooth pipes with the experimental values of Bogue	40
4.6	Comparison of pressure drops obtained using various annular flow equations to calculate the pressure gradient using an example in Skelland (1967)	44

List of Figures

Figure		Page
4.1	Schematic diagram of wellbore	9
4.2	Mesh centred grid representing the wellbore. (schematic)	14
4.3	30 x 30 coefficient band matrix from 3 x 10 block matrix using standard ordering	16
4.4	Initial and boundary conditions	17
4.5	30 x 21 band storage matrix from 30 x 30 band matrix	20
4.6	Variation in f with roughness height for pipe radius of 3 inches	38
5.1	Comparison of annular temperature profiles	48
5.2	Effect of heat generation on the annulus temperature profile	51
5.3	Comparison of steady state and unsteady state annulus temperature profiles	56
5.4	Effect of variations in the mud heat capacity on the annulus temperature profile	58
5.5	Effect of variations in the mud density on the annulus temperature profile	60
5.6	Effect of allowing for the cuttings density on the annulus temperature profile	61
5.7	Effect of variations in the mud flow rate on the annulus temperature profile	63
5.8	Effect of variations in the geothermal gradient on the annulus temperature profile	64
5.9	Effect of variations in the thermal conductivity of the earth on the temperature profile	65
5.10	Effect of variations in the hydraulic radius on the annulus temperature profile	67
5.11	Effect of variations in the inlet fluid temperature on the annulus temperature profile	68

5.12 Approximation of annulus temperature profile to initial conditions after 24 hours flow 71

Nomenclature

A, B, C	constants in the Robertson and Stiff rheological model (Equation 4.17)
An	drill bit nozzle area, ft^2
C_p	heat capacity of drilling fluid, Btu/lb-°F
D	internal diameter of pipe, ft
e	mechanical efficiency
E	energy, Btu/hr-ft
f	Fanning friction factor
g	acceleration due to gravity, ft/hr^2
g_c	conversion factor, 416.975×10^6 lbm-ft/lbf-hr^2
Gz	Graetz number, $C_p q\rho/kL$, dimensionless
h	convective heat transfer coefficient, Btu/ft^2-hr-°F
HP	horsepower
K	thermal conductivity, Btu/ft^2-hr-°F
K	fluid consistency index, lbm/hr^2-ft
K′	Metzner and Reed power law coefficient, lbf-hr-ft^{-2}
L	length, ft
m	geothermal gradient, °F/ft
n	time level, dimensionless
n′	flow behaviour index, dimensionless
n′′	Metzner and Reed modified power law exponent, dimensionless
N	number of vertical elements
Nu	Nusselt number, hD/K, dimensionless
Pr	non-Newtonian Prandtl number, dimensionless (Equation 4.19)

q	fluid flow rate, ft^3/hr
Q	heat generation term, Btu/hr-ft
r	radius, ft
Re	non-Newtonian Reynolds number, dimensionless (Equation 4.22)
Re_c	critical Reynolds number, dimensionless (Equation 4.23)
$Re_{(gen)}$	generalized Reynolds number, dimensionless (Equation 4.21)
St	Stanton number, $h/\rho C_p V$, dimensionless
T	temperature, °F
Tmi	inlet fluid temperature, °F
Ts	surface temperature, °F
V	velocity, ft/hr
x	drilling rate, ft/min
z	depth, ft
Z	distance traveled up annulus by an element of fluid in 1 minute, ft
ΔP	pressure drop, lbf/ft^2
ε	roughness height, in.
γ	shear rate, hr^{-1}
ρ	density of drilling fluid, lbm/ft^3
μ	viscosity, lbm/ft-hr
η	plastic viscosity, lbm/ft-hr
τ	shear stress, lbf/ft^2
τ_y	yield stress, lbf/ft^2

Subscripts:

a	annulus; inner annular wall
b	drill bit
e	external limit
f	formation
i, j	radial and vertical elements, respectively
jmx	maximum vertical element
o	outer annular wall
p	drill pipe
w	drill pipe wall

1. INTRODUCTION

Today the drilling of a well to depths approaching 30,000 feet on land, and offshore in water depths of several thousands of feet, is becoming increasingly commonplace. This, coupled with the fact that the search for oil is being concentrated in the hostile environments of such areas as the North Sea and the High Arctic, has made the drilling of a well a highly complicated and expensive operation.

With such enormous costs and the highly advanced technology involved, it is necessary that the most efficient means possible be employed in the drilling of oil wells. Hence, accurate procedures for estimating the numerous variables involved are becoming essential, both at the design stage and at the wellsite, even though the complicated nature of some of these variables would mean the development of intricate models.

Although various models have been formulated to enable certain parameters to be estimated, most have been oversimplified so as to enable their use at the wellsite in the form of simple equations, solvable by a sliderule, nomographs or plots. As a result the practical application of the relevant theory is minimal. In the present era of powerful minicomputer systems, this can no longer be justified and it is becoming increasingly more feasible to utilize the complicated theory that exists in the literature, at the wellsite. Models developed from such

theory, with subsequent improvements in accuracy, are probably most useful at the well planning and design stage in view of the fact that large powerful computers are available with virtually no limitations on solution time or storage space, for all practical purposes.

One of the parameters, of which a thorough knowledge would be very helpful, is temperature. In the past it has been convenient to ignore the temperature distribution in a well and to assume an isothermal system, primarily because no practical means existed for determining the wellbore temperature profile. An accurate means of estimating the temperature distribution, and its variation with time, would have a variety of applications as follows:

1. Enable the dynamic temperature profile and bottomhole temperature to be determined rather than the static temperatures presently available from electric logging tools.
2. Improve cementing programme design, particularly with regard to the amount of retarder required, and the setting time.
3. Improve drilling fluid design by providing information on the actual circulating temperatures so as to enable high temperature modifications to be made to the drilling fluid programme.
4. Enable casing thermal stresses to be determined.
5. Provide improved well design in permafrost regions.
6. Improve injection and production operations.

At the present time the only temperature information available at the wellsite is the inlet and outlet fluid temperatures and the static bottomhole temperature obtained from a logging tool. The purpose of this dissertation is to employ the existing theory in the literature on transient heat flow in a wellbore to develop a computer model to estimate the temperature distribution and its variation with circulating time. Unlike previous models, it will be feasible to use this model at a remote wellsite without a significant loss of accuracy. Furthermore this model incorporates a number of improvements over previous models in terms of both accuracy and applicability.

A further aim of this study was to use the computer model to simulate wellbore temperature distributions so that a complete parametric sensitivity analysis could be carried out to indicate which parameters have the most significant effect on the temperature.

2. REVIEW OF THE AVAILABLE MODELS

Temperature distribution in a wellbore is a complicated function of a large number of variables, many of which are not known with any degree of certainty. For this reason, any mathematical model must contain simplifying assumptions to enable a solution to be obtained. The more complicated the model, the more data are required. In view of the fact that any model can only be as accurate as the data that it uses, the intricacy of the model is not in itself a sufficient criterion for accuracy.

A number of models exist for estimating bottomhole temperatures and wellbore temperature distributions in the literature. Some of these have been designed for practical application, and each includes a variety of simplifying assumptions. The earlier, hand-solved methods tend to be the most simplified and inaccurate.

The bottomhole temperature charts developed by Farris (1941) were based solely on measurements of the circulating temperatures in five shallow Gulf Coast wells. Despite the obvious inaccuracies and oversimplifications involved in the use of the Farris charts, and their restrictive application, the API recommends them for determining setting schedules for cement slurries. The severe shortcomings of these charts prompted research into a more accurate, mathematical method for estimating circulating temperatures.

Edwardson et al. (1962) solved the differential heat conduction equations to estimate the formation temperature distribution before and after circulation. However, this work was more concerned with temperature distribution in the formation as a result of drilling fluid circulation, and does not allow the direct calculation of the wellbore temperature distribution. Moreover, assumed formation temperature profiles were used at the end of circulation.

Tragesser et al. (1969) expanded Edwardson's method so as to allow for such variables as depth, pump rate, hole size and so forth, but their method involved the same limiting assumptions.

Holmes and Swift (1970) assumed steady state conditions in the wellbore and surrounding formation, and solved the relevant heat transfer equations analytically, using this assumption. This method has the advantage of being simple and more accurate than previous methods, but the assumption of steady state heat flow is a critical one which is only satisfied after impractically long circulation times.

In terms of the theoretical development of the heat transfer relationships for a wellbore, the work of Raymond (1969) is the most comprehensive. It is this work that has served as a basis for all the recent research on the subject. He advocated the use of the principle of superposition and the Hurst and van Everdingen functions to solve numerically for unsteady state conditions. However, he contended that the pseudo-steady state condition was

accurate enough for all practical purposes and described an analytical means of solving for this condition.

Most recent research has dealt with means of solving the unsteady state equations formulated by Raymond, or variations on these, using finite difference techniques, e.g. Sullivan (1970), Keller et al. (1973), Sump and Williams (1973) and Oster (1976). The approach of Keller et al. is the most comprehensive of these methods. As well as solving the finite difference equations, variations in the wellbore geometry were included. A further refinement was the allowance for heat generation within the fluid column due to friction forces and the rotational energy.

It is the work of Keller et al., which itself is an extension of Raymond's work, that is the basis of this research.

3. STATEMENT OF THE PROBLEM

A review of the literature on determining static and dynamic wellbore temperature distributions suggests that a compromise must be made between accuracy and time required to obtain the temperature distribution. The early methods are inaccurate but the temperature data is readily acquired; the more recent ones are quite accurate but necessitate impractically long periods of time to obtain solutions.

A need exists for a method that is both accurate and fast thus enabling it to be used at the wellsite where it would be of greatest value. Such an application is not possible with any of the existing means of obtaining dynamic temperature data, without sacrificing accuracy.

This dissertation utilizes the existing theory on the subject of wellbore transient heat transfer to develop a computer model that is both accurate, and by means of a direct solution technique, much faster than previous mathematical methods.

The study also investigated the effect of considering the non-Newtonian flow behaviour of the circulating medium on the temperature profiles generated by the model.

4. THEORY AND DEVELOPMENT OF THE MODEL

The physical system, upon which this computer model is based, is shown schematically in Fig. 4-1

The flow of a drilling fluid in a wellbore may be divided into three distinct regions as follows:

1. Downward flow through the drill string.
2. Flow from the drill string through the drill bit into the annulus.
3. Upward flow through the annulus.

The temperature of the fluid in each region is dependent upon a number of different thermal processes. The fluid enters the drill pipe with a known temperature and its change in temperature is determined by the rate of thermal convection down the fluid column and the rate of convective heat transfer radially between the fluid, the pipe wall and the annulus. Vertical and radial heat conduction within the pipe wall is also present.

As the fluid flows up the annulus, its temperature is dependent upon the rate of heat convection up the annulus, the rate of radial convection between the annulus fluid, the drill pipe wall and the fluid within the drill pipe, the rate of radial convection between the annulus fluid and the formation or casing and the conduction through the formation.

Since transient heat transfer is considered, the time of circulation has an important effect on the temperature of

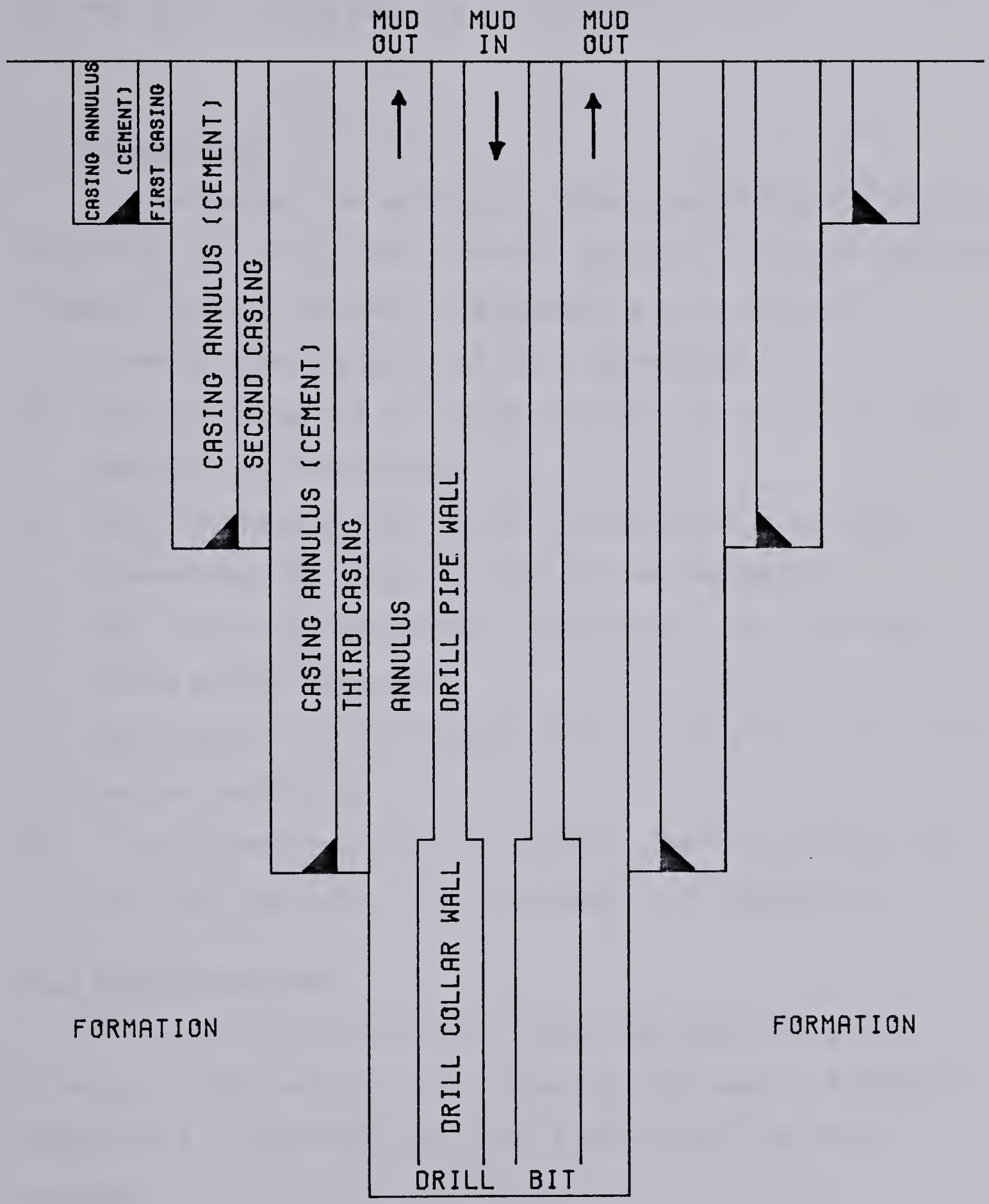


FIG.4-1: SCHEMATIC DIAGRAM OF WELL.
FOR DIMENSIONS SEE TABLE 4-1

the fluid as has the heat generation within the three flow regions due to frictional forces and the rotational energy of the drill string and the drill bit.

4.1 Assumptions

To arrive at the energy balances describing the thermal behaviour of the wellbore certain assumptions about the heat transfer mechanisms and flow behaviour are required.

1. Flow is steady state and fully developed.
2. Flow is turbulent in the drill pipe and drill bit and laminar in the annulus.
3. Heat transfer within the drilling fluid is by axial convection. Axial conduction may be neglected.
4. The radial temperature gradient within the drilling fluid may be neglected.
5. Heat generation by viscous dissipation within the fluid may be neglected.
6. Fluid properties such as density, thermal conductivity and heat capacity, are independent of temperature.

4.2 Energy Balances

The partial differential equations describing the energy balances within the system are derived in Appendix I. Equation 4.1 describes the heat flow within the drill string.

$$\rho q C_p \frac{\partial T_p}{\partial z} + 2\pi r_p h_p (T_p - T_w) = -\rho C_p \pi r_p^2 \frac{\partial T_p}{\partial t} + Q_p \qquad (4.1)$$

The terms on the left represent the vertical and radial convective heat transfer, respectively. The right hand terms represent the accumulation of energy within the drill string and the energy sources, respectively.

The energy balance in the drill pipe wall is given by Equation 4.2.

$$k_w \frac{\partial^2 T_w}{\partial z^2} + \frac{2 r_p h_p}{(r_a^2 - r_p^2)} (T_p - T_w) + \frac{2 r_a h_a}{(r_a^2 - r_p^2)} (T_a - T_w) = \rho_w C_{pw} \frac{\partial T_w}{\partial t} \qquad (4.2)$$

The first term on the left hand side represents the vertical heat conduction within the wall. The second and third terms account for the radial heat transfer to the drilling fluid inside and outside the wall. The right hand term represents the heat accumulation.

The energy balance in the flow annulus is expressed by Equation 4.3.

$$\rho q C_p \frac{\partial T_a}{\partial z} + 2\pi r_a h_a (T_w - T_a) + 2\pi r_o h_o (T_f - T_a) = \rho C_p \pi (r_o^2 - r_a^2) \frac{\partial T_a}{\partial t} \qquad (4.3)$$

The three left-hand terms represent the vertical convective heat transfer within the fluid, radial convection between the drilling fluid and the drill pipe wall and radial convection between the drilling fluid and the casing or formation, respectively. Heat accumulation and generation are accounted for by the two right-hand terms.

Equation 4.4 is a two-dimensional thermal conductivity

$$\frac{\partial^2 T_f}{\partial z^2} + \frac{\partial^2 T_f}{\partial r^2} + \frac{1}{r}\frac{\partial T_f}{\partial r} = \frac{\rho_f C_{pf}}{k_f}\frac{\partial T_f}{\partial t} \qquad (4.4)$$

equation representing heat flow in the formation. The two left-hand terms account for the vertical and radial conduction, and the right-hand term accounts for the heat accumulation.

Since the original, theoretical work of Raymond (1969) on this subject, these equations have formed the basis of the various thermal wellbore models that have been developed. Prior to Raymond's work the thermal models were all very simplified to the extent that they were of little value in estimating the temperature distribution with any degree of accuracy.

4.3 Solution of the Partial Differential Equations.

The solution of these equations to obtain a temperature distribution as a function of time is complicated and the models developed subsequent to Raymond's paper incorporated solution methods based on finite difference techniques. The

solution of these finite difference equations all involved iterative methods with the obvious disadvantages of long solution times and the concurrent problems of stability and accuracy. Keller et al. (1973), whose work on the subject is the most comprehensive to date, quote a solution time of 170 seconds on a CDC 6400 for a sample problem. Obviously such a method is impractical for any wellsite application.

In the present solution method, the wellbore and the adjacent formation are represented by a two-dimensional, mesh-centred grid consisting of ten radial elements and a variable number of vertical elements depending on the well depth, but approximately one element for each 100 feet of depth. Each of the radial elements corresponds to a different portion of the wellbore cross-section from the centre of the drill string into the formation, as shown in Fig. 4-2. The ten radial elements allow for a well profile with up to three casing strings and the resulting mesh-centred grid is of a form similar to that in Fig. 4-2. Using this grid as a basis, the above partial differential equations can be written in finite difference form for each element of the grid so as to describe the transient heat flow in that element. The finite difference equations are written in an implicit form and are derived in their general form in Appendix II. Two-point forward and two-point backward difference approximations are used to represent the first order spatial derivatives and the time derivatives. The second order spatial derivatives are represented by

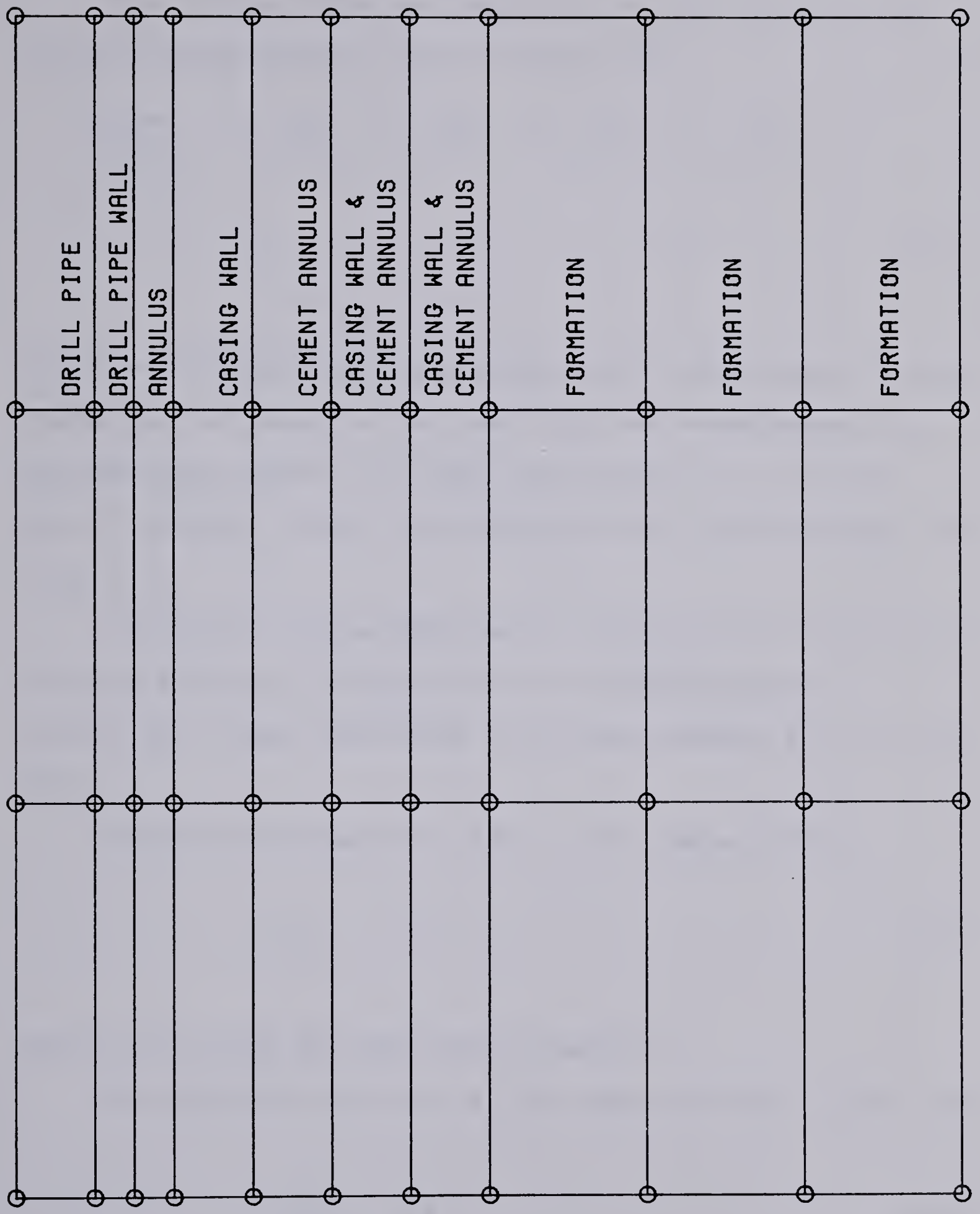


FIG.4-2: MESH CENTRED GRID REPRESENTING THE WELLBORE. (SCHEMATIC)

three-point central difference approximations.

The finite difference equations may be arranged into the following general form for each node.

$$B_{ij}T^{n+1}_{i,j-1} + D_{ij}T^{n+1}_{i-1,j} + E_{ij}T^{n+1}_{i,j} + F_{i,j}T^{n+1}_{i+1,j} + H_{ij}T^{n+1}_{i,j+1} = C_{ij} \qquad (4.5)$$

Using a standard ordering procedure the coefficients in the above general equation for each node are represented by a pentadiagonal matrix, so that the original N x 10 block matrix becomes a 10N x 10N band matrix of the form shown in Fig. 4-3.

Having set up the band matrix, certain modifications to it are required to satisfy the initial and boundary conditions. These conditions are shown schematically in Fig. 4-4.

Equation 4.6 describes the initial temperature

$$T^{1}_{i,j} = Ts + mz_j \qquad (4.6)$$

profile as being the geothermal gradient.

The boundary condition at the upper surface is given by

$$\left.\frac{\partial T}{\partial z}\right|_{z=0} = 0 \qquad (4.7)$$

Equation 4.7, which indicates no flow of heat between the

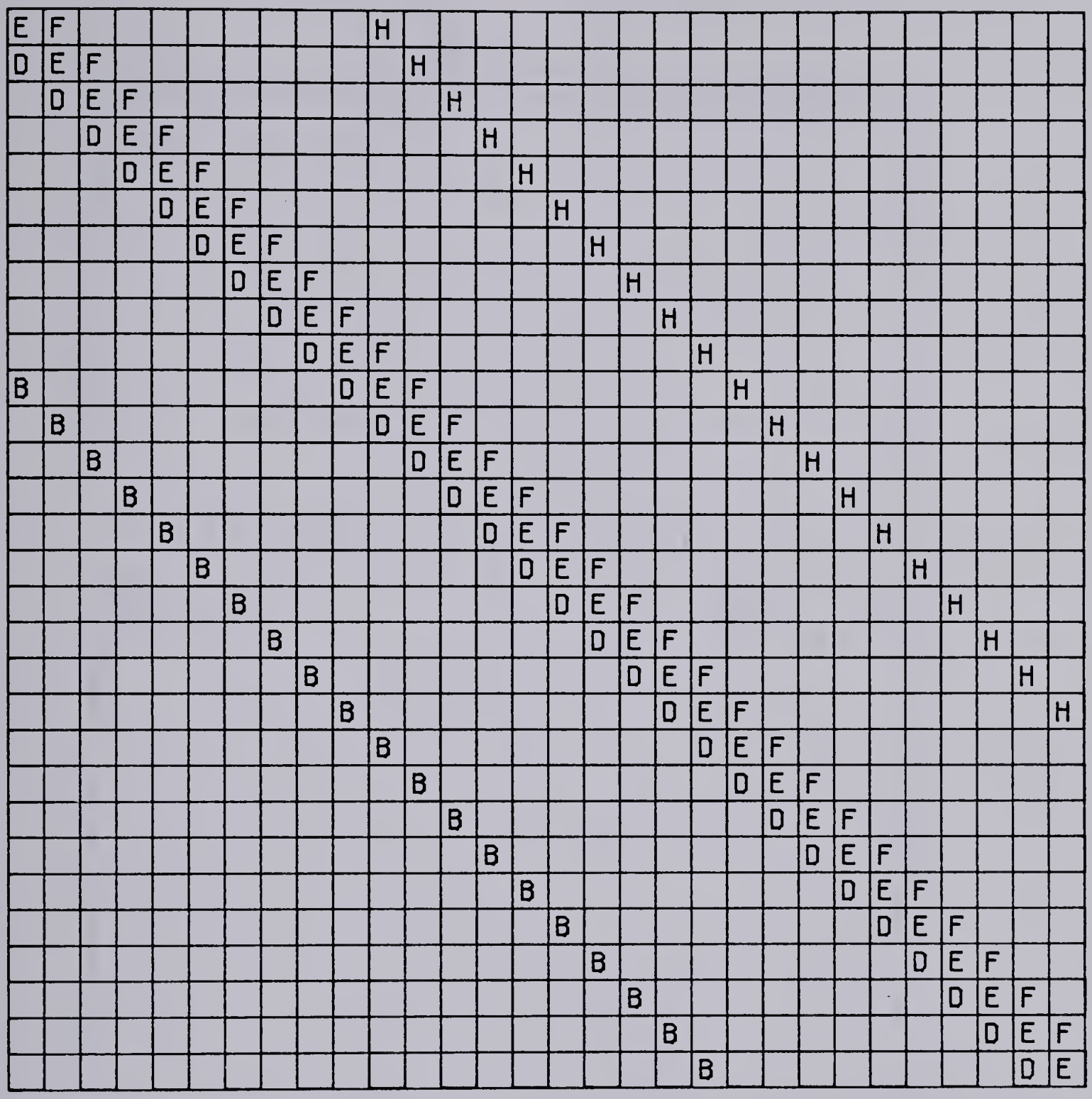


FIG.4-3: 30 X 30 COEFFICIENT BAND MATRIX FROM 3 X 10 BLOCK MATRIX USING STANDARD ORDERING

$$\left.\frac{\partial T}{\partial z}\right|_{z=0} = 0$$

$$T^{n}_{1,0} = T_{mi}$$

$$\left.\frac{\partial T}{\partial r}\right|_{r=0} = 0 \qquad \left.\frac{\partial T}{\partial r}\right|_{r=r_e} = 0$$

$$T^{1}_{i,j} = Ts + mz_j$$

$$T^{n}_{1,jmx} = T^{n}_{2,jmx} = T^{n}_{3,jmx}$$

$$T^{n}_{i,jmx+1} = Ts + mz_{jmx+1}$$

FIG.4-4: INITIAL AND BOUNDARY CONDITIONS.

earth and the atmosphere.

The inner and outer radial boundary conditions are described by Equations 4.8 and 4.9.

$$\left.\frac{\partial T}{\partial r}\right|_{r=0} = 0 \tag{4.8}$$

$$\left.\frac{\partial T}{\partial r}\right|_{r=r_e} = 0 \tag{4.9}$$

These equations imply that no heat flows across these boundaries.

Equation 4.10 denotes the inlet fluid temperature as

$$T^n_{1,0} = T_{mi} \tag{4.10}$$

being the boundary condition at the innermost upper element.

The boundary condition along the lower surface is given in Equation 4.11.

$$T^n_{i,jmx+1} = Ts + mz_{jmx+1} \tag{4.11}$$

Equation 4.12 ensures that the temperatures are equalized at the drill bit.

$$T^n_{1,jmx} = T^n_{2,jmx} = T^n_{3,jmx} \tag{4.12}$$

Because of this final condition, the band matrix must be modified slightly by "folding in" the H coefficients of the

second and third radial elements of the final row. To achieve this, two extra lower co-diagonals are required, each with one of the coefficients. The matrix in its final form, incorporating the initial and final boundary conditions, is an asymmetric, heptadiagonal band matrix.

Because of the potentially large storage requirements of such a matrix, especially where a deep well is being modeled, it is transformed into a band storage matrix of the form shown in Fig. 4-5, thus reducing its size from 10N x 10N to 10N x 23. This band storage matrix is then solved by a direct band algorithm technique involving factorization into lower and upper triangular matrices. The details of this method are adequately covered in the literature e.g. Peaceman (1973), and will not be considered here. The actual solution was achieved by means of an IMSL subroutine LEQT1B, and is described in more detail in Appendix III.

When the band algorithm, direct solution method was used for the test data in Table 4-1, the resulting annulus temperature profile was identical to that of Keller et al. (1973). However, instead of requiring a solution time of 170 seconds on a CDC 6400, about 3 seconds were needed on an Amdahl 470.

4.4 The Selection of an Appropriate Rheological Model

The basis of any model of the drilling process is the drilling fluid or mud. The drilling fluid serves a variety of purposes such as cooling the bit, transporting formation

										E	F									H
									D	E	F									H
									D	E	F									H
									D	E	F									H
									D	E	F									H
									D	E	F									H
									D	E	F									H
									D	E	F									H
									D	E	F									H
									D	E	F									H
B									D	E	F									H
B									D	E	F									H
B									D	E	F									H
B									D	E	F									H
B									D	E	F									H
B									D	E	F									H
B									D	E	F									H
B									D	E	F									H
B									D	E	F									H
B									D	E	F									H
B									D	E	F									
B									D	E	F									
B									D	E	F									
B									D	E	F									
B									D	E	F									
B									D	E	F									
B									D	E	F									
B									D	E	F									
B									D	E	F									
B									D	E	F									
B									D	E										

FIG.4-5: 30 X 21 BAND STORAGE MATRIX
FROM 30 X 30 BAND MATRIX.

TABLE 4.1: REFERENCE DATA FOR THE WELLBORE THERMAL MODEL.

Drill Pipe ID (in.)	5.965
Drill Pipe OD (in.)	6.625
Drill Collar ID (in.)	2.750
Drill Collar OD (in.)	6.750
First Casing ID (in.)	19.124
First Casing OD (in.)	20.000
Second Casing ID (in.)	12.515
Second Casing OD (in.)	13.375
Third Casing ID (in.)	8.835
Third Casing OD (in.)	9.625
Total well diameter (in.)	26.000
Open hole diameter (in.)	8.375
Total Depth (ft)	15000
Depth to top of Drill Collars (ft)	13000
Depth of First Casing Shoe (ft)	2000
Depth of Second Casing Shoe (ft)	5000
Depth of Third Casing Shoe (ft)	10000
Depth to Cement - First Csg. Annulus (ft)	0
Depth to Cement - Second Csg. Annulus (ft)	1000
Depth to Cement - Third Csg. Annulus (ft)	4500

	DENSITY lb/cu ft	HEAT CAP. Btu/lb-F	THERMAL COND. Btu/hr-ft-F
Drill Pipe	487.00	0.1	25.0
Drill Collars	556.00	0.1	25.0
Casing	503.00	0.1	25.0
Drilling Fluid	74.81	0.4	1.0
Cement	196.00	0.5	0.4
Earth	165.00	0.2	1.3

Flow rate (cu ft/hr)	= 1685
Surface temperature (deg.F)	= 59.5
Geothermal Gradient (deg.F/ft)	= 0.0127

cuttings to the surface and controlling subsurface pressures. It is here that a fundamental question arises - how to best model the drilling fluid rheology? Drilling fluids have progressed from being little more than clay suspensions to highly complex substances both rheologically and chemically. This is further compounded by the fact that the rheology and chemistry can vary enormously, even during the course of drilling a single well, depending on prevailing circumstances. Obviously some form of consistency must be utilized, at the cost of accuracy, as it is completely unfeasible to design a drilling fluid programme incorporating all the vagaries of the rheology and chemistry of the mud.

The only valid generalization about drilling fluids is that they are non-Newtonian. Even so, several early workers on the subject e.g. van Olphen (1950) and Cardwell (1953) assumed them to be Newtonian, probably due to the fact that very little was known of non-Newtonian fluid behaviour. Unlike Newtonian fluids,which have the constitutive equation

$$\tau_{rz} = -\frac{\mu}{g_c}\frac{dV_z}{dr} \qquad (4.13)$$

no single constitutive equation exists to describe exactly the relationship between the shear stress and shear rate of all non-Newtonian materials over all ranges of shear rates. Even if such an equation could be developed its intricacy would defy engineering application. Slawomirski (1975) has

derived a constitutive equation for time independent drilling fluids which illustrates this. Although three major categories of non-Newtonian systems are recognized, namely, time independent, time dependent and viscoelastic, only the time independent system has received any degree of study. Fortunately the large majority of industrial non-Newtonian fluids, including drilling fluids, fall into this category. The time independent fluids can be further subdivided into Bingham plastic, pseudoplastic and dilatant fluids. Numerous simplified empirical "models" have been developed to relate the shear stress to the shear rate for these fluids, especially the pseudoplastics which constitute the largest and probably the most important class of non-Newtonian fluids. Skelland (1967) has summarized the most important of these equations and the diversity of drilling fluids is such that a particular type of drilling fluid probably exists that would be described by each of these models. Slawomirski (1975) contends that the majority of drilling fluids are thixotropic, but the equations to describe such behaviour are so complicated as to be inapplicable to engineering problems. Hence it is generally accepted that drilling fluids are typified by either the Bingham plastic

$$\tau_{rz} = \tau_y + \frac{\eta}{g_c}\left(-\frac{dV_z}{dr}\right) \qquad (4.14)$$

or Ostwald-deWaele power law models.

$$\tau_{rz} = \frac{K}{g_c}\left(-\frac{dV_z}{dr}\right)^{n'} \qquad (4.15)$$

This simplified linearized version of the former was very much in favour until the past decade when the advent of complicated polymer muds and the expanding use of oil base muds emphasized the need for the power law model. The power law model is easily applied and hence the large majority of the research on non-Newtonian flow utilizes this model as best typifying pseudoplastics. Bingham plastic fluids, on the other hand, are found only rarely, although high solids drilling fluids are well described by this model.

When the functions of a drilling fluid are considered it is obvious that a pseudoplastic would be the most appropriate type of fluid. It is shear thinning so that at the high shearing rates present at the bit, the pressure drop is minimized, whereas at the low shear rates in the annulus the viscosity is increased, thus enabling the large volume of cuttings to be efficiently removed.

However, using the power law model is more a matter of convenience than of theoretical validity, as it has certain disadvantages. Drilling fluids typically possess a yield value which cannot be accounted for by this model. Furthermore the power law model predicts infinite viscosities and zero viscosities in the limits of very low and very high shear rates, respectively. Real fluids,

however, exhibit a finite and constant viscosity at zero shear rate. The use of this model also requires that the two defining parameters K and n' remain constant over the entire range of shear stress. Fortunately these limitations appear to be unimportant for drilling applications, if the drilling fluid properties are assumed independent of temperature.

Nonetheless some have considered these constraints as justification for the use of the Bingham plastic model and it is still used today despite its limitations being much more significant than those of the power law model. The Bingham model accounts for the yield values typical of most drilling fluids, but it assumes a linear relationship between shear stress and shear rate after an initial yield, something that is not true of drilling fluids. Another negative feature is that no explicit relationship can be derived between the shear stress and the volumetric flow rate. Furthermore the form used is a simplified, linearized version first proposed by Caldwell and Babbit (1941) and the simplification has been shown to be erroneous under certain circumstances by Hanks and Pratt (1967). However, the simplified model is still used, particularly in drilling hydraulics, without any regard to the limitations.

Recently attempts have been made to resolve the controversy by proposing models that combine the obvious shear thinning features of drilling fluids with a yield stress. The Herschel-Bulkley model

$$\tau_{rz} = \tau_y + \frac{K}{g_c}\left(-\frac{dV_z}{dr}\right)^{n'} \qquad (4.16)$$

has been considered but its application at the wellsite is difficult due to the intricacy of the equations describing the flow behaviour and the fact that no explicit relationship exists between the shear stress and the volumetric flow rate for this model. Zamora and Bleier (1977) have advocated the use of a simplified version of this model and Robertson and Stiff (1976) derived an original model for a yield-pseudoplastic

$$\tau_{rz} = A\left(-\frac{dV_z}{dr} + C\right)^B \qquad (4.17)$$

that has certain advantages over the Herschel-Bulkley model.

Whilst recognizing the attractiveness of the yield-pseudoplastic category for drilling fluids, little work has been done on the equations necessary to describe the behaviour of such a fluid in the wellbore. For this work it is proposed to use the power law model as being the best overall compromise, and primarily because the vast majority of the relevant theory in the literature is based upon this model.

4.5 Non-Newtonian Convective Heat Transfer Coefficients

The non-Newtonian behaviour of drilling fluids is something that all previous publications on the subject of wellbore temperature distribution have ignored. No mention is made of any investigations to ascertain the effect of the pseudoplasticity of a drilling fluid on the convective heat transfer coefficients.

All previous work on this subject has used the conventional Sieder-Tate correlation to estimate the convective heat transfer coefficients, including Raymond (1969) and Keller et al. (1973). Sump and Williams (1973), whilst recognizing that the use of the Sieder-Tate correlations resulted in anomalously low temperatures, modified this correlation by regressing on temperature data from six Gulf Coast wells. Their empirical relationship resulted in modified heat transfer coefficients which they claim give improved temperature profiles. However, the fact that data from only six wells were used makes their relationship highly suspect for general use.

Inherent in the use of the Sieder-Tate correlation is the assumption that flow is turbulent. Whilst this is generally the case within the drill string, it is seldom true in the annulus. Thus, the use of the Sieder-Tate correlation, even with the assumption of non-Newtonian flow, is invalid for determining annulus convective heat transfer coefficients.

Given the shortcomings of the previous work on wellbore

temperature distributions with regard to the convective heat transfer coefficients used, an investigation was carried out to compare the heat transfer coefficients obtained from non-Newtonian correlations with the Sieder-Tate values, and to determine how significant is the difference between the resulting coefficients.

An extensive review of the literature on the subject of non-Newtonian convective heat transfer coefficients revealed a remarkable dearth of research in this area. Such relationships that do exist are either purely empirical and relatively simple, or analytical and invariably very complicated. The latter usually allow for the nonisothermal nature of such parameters as heat capacity, but their intricacy makes their use impractical for the application envisaged in this study. However, the empirical nature of the simple relationships, which would be ideally suited to this thermal model, means that each relationship gives a different result, and no independent criterion exists to determine which is the most accurate.

The convective heat transfer coefficients obtained from the correlations that would be of use in this study are summarized in Tables 4-2, 4-3 and 4-4 for turbulent pipe flow, laminar annular flow and laminar pipe flow, respectively. These are all empirical or semi-empirical relationships, and none of the analytical relationships have been included.

It is evident from Table 4-2 that the Lakshminarayanan

TABLE 4.2: COMPARISON OF NON-NEWTONIAN CONVECTIVE HEAT TRANSFER COEFFICIENTS FOR TURBULENT PIPE FLOW OF POWER LAW FLUIDS.

(1) Lakshminarayanan et al. (1976)

(2) Clapp (1961)

(3) Non-Newtonian Sieder-Tate

(4) Metzner and Friend (1959)

				h (Btu/hr-ft²-°F)			
n′	K	Re	Pr	(1)	(2)	(3)	(4)
0.55	0.1586	2649	48.7	101.2	81.0	108.5	17.0
0.60	0.1321	2675	48.3	101.6	84.1	109.0	22.1
0.65	0.1100	2703	47.8	101.9	87.7	109.6	27.3
0.70	0.0916	2733	47.3	102.3	91.9	110.1	32.3
0.75	0.0763	2764	46.7	102.7	96.5	110.7	37.1
0.80	0.0635	2796	46.2	103.1	101.5	111.3	41.7
0.85	0.0529	2829	45.7	103.5	106.9	111.9	46.0
0.90	0.0441	2863	45.1	103.9	112.6	112.5	50.0
0.95	0.0367	2898	44.6	104.4	118.7	113.2	53.7

TABLE 4.3: COMPARISON OF NON-NEWTONIAN CONVECTIVE HEAT TRANSFER COEFFICIENTS FOR LAMINAR ANNULAR FLOW OF POWER LAW FLUIDS (INNER AND OUTER WALLS RESPECTIVELY).

(1) Skelland (1967)

(2) Tanaka and Mitsuishi (1975)

n′	NUSSELT NO. (1)	(2)	h (Btu/hr-ft²-°F) (1)		(2)	
0.55	4.04	3.53	7.32	5.79	6.39	5.05
0.60	4.03	3.55	7.29	5.77	6.43	5.09
0.65	4.01	3.58	7.26	5.75	6.48	5.13
0.70	4.00	3.60	7.24	5.72	6.52	5.16
0.75	3.98	3.63	7.21	5.71	6.57	5.20
0.80	3.97	3.65	7.19	5.69	6.61	5.23
0.85	3.96	3.68	7.17	5.67	6.66	5.27
0.90	3.95	3.70	7.16	5.66	6.70	5.30
0.95	3.94	3.72	7.14	5.65	6.74	5.33

Criterion for Nusselt No. (2) : > 9.1

Annular Length = 1000 ft

TABLE 4.4: COMPARISON OF NON-NEWTONIAN NUSSELT NUMBERS FOR LAMINAR PIPE FLOW OF POWER LAW FLUIDS.

(1) Metzner (1965)

(2) Charm and Merrill (1959)

(3) Mizushina and Kuriwaki (1968)

(4) Bird (1959)

(5) Grigull (1956)

(6) Skelland (1967)

	NUSSELT NOS.					
n′	(1)	(2)	(3)	(4)	(5)	(6)
0.55	6.88	8.16	72.51	4.68	4.16	4.28
0.60	6.81	7.99	64.71	4.63	4.18	4.25
0.65	6.74	7.86	58.50	4.58	4.21	4.23
0.70	6.69	7.75	53.47	4.54	4.23	4.20
0.75	6.64	7.66	49.32	4.50	4.25	4.19
0.80	6.60	7.59	45.85	4.47	4.28	4.17
0.85	6.56	7.53	42.92	4.44	4.30	4.15
0.90	6.52	7.48	40.41	4.41	4.32	4.14
0.95	6.49	7.43	38.24	4.39	4.34	4.13

Pipe Length = 1000 ft

et al. (1976) and the non-Newtonian Sieder-Tate values compare favourably with the Newtonian Sieder-Tate value of 113 Btu/hr-ft²-°F if the value of n′ is assumed to be between 0.7 and 0.8, a typical value. The correlation of Clapp (1961) has been criticized by Metzner (1965) for experimental errors, which probably explains the discrepancies in Table 4-2. The relationship of Metzner and Friend (1959) is invalid in this particular study because the necessary criterion (Equation 4.18) is not satisfied.

$$\frac{RePr}{n'^{0.25}}\sqrt{\frac{f}{2}} > 5000 \qquad (4.18)$$

where

$$Pr = \frac{KC_p}{k}\left(\frac{3n'+1}{4n'}\right)^{n'}\left(\frac{8V}{D}\right)^{n'-1} \qquad (4.19)$$

Table 4-3 indicates a favourable comparison between the non-Newtonian Nusselt numbers and the Newtonian value of 4.12 for laminar flow quoted by Keller et al. (1973). This is also the case in Table 4-4 where the use of laminar pipe flow correlations is justified by neglecting the radial temperature gradient. Thus, the Nusselt number will be the same for both the inner and outer annular walls. Several of these correlations, namely Tanaka and Mitsuishi (1975), Metzner (1965) and Charm and Merrill (1959), involve the Graetz number which means that the Nusselt number becomes length dependent. Since the typical dimensions of a wellbore ensure that the flow is fully developed, such correlations

are unsuitable. The discrepencies in the values determined from the correlation of Mizushina and Kuriwaki (1968) are propably due to the fact that they based their experiments on CMC solutions, which are viscoelastic, not pseudoplastic.

As indicated in chapter 5, variations in the convective heat transfer coefficients have no significant effect on the annular temperature profile. Thus, the use of Newtonian heat transfer coefficients is valid. However, the relationship of Lakshminarayanan et al. (1976) was used in this study for theoretical completeness and because it is the most recent correlation. This relationship is given in Equation 4.20.

$$St = 0.0107Re^{-0.33} Pr^{-0.67} \qquad (4.20)$$

The value of 4.12 was used for annular Nusselt numbers.

4.6 Calculation of the Energy Source Terms

The heat generation within the system is the result of several different energy sources namely:

1. Rotational energy due to the work required to rotate the drill string.
2. The work done by the drill bit.
3. Viscous energy due to the friction losses inside the drill pipe, drill bit and annulus.

The calculation of the thermal energy due to the first two sources is achieved by assuming that all the mechanical energy input by the rotary drive is converted to thermal

energy along the length of the drill pipe. Keller et al. (1973) divided this energy 60% to 40% between the drill pipe and the drill bit, respectively.

Thus, these terms will be dependent upon each individual drilling rig, and would be calculated by a simple relationship between the rotating speed of the string, and the rotary horsepower required to maintain this speed. The horse power would be converted directly to thermal energy.

The determination of the energy terms, resulting from the frictional presure losses within the system, is more difficult. To calculate the energy input due to the frictional pressure losses, it is necessary to first determine these losses in the drill string, drill bit and annulus, which in turn, requires relationships between the pressure drop and the known flow parameters and geometry.

It has already been shown that the rheology of drilling fluids is adequately represented by the Ostwald deWaele power law model. Therefore, the appropriate relations for determining the frictional pressure losses for power law fluids are used in the model. Unfortunately, there are a number of such relations in the literature, and it is necessary to select the ones most applicable to this particular model.

An assumption already made is that flow is turbulent in the drill pipe and laminar in the annulus. A method is included in the model to verify that this assumption is valid for the flow conditions pertaining at any particular

time. The traditional criterion for establishing this is to compare the Reynolds number with a value of 2100. The Reynolds number used is that derived by Metzner and Reed (1955) for time independent, non-Newtonian fluids.

$$Re_{(gen)} = \frac{D^{n''} V^{2-n''} \rho}{g_c K' 8^{n''-1}} \qquad (4.21)$$

This may be readily modified to apply to pseudoplastic fluids on the assumption that n′ and K remain constant.

$$Re = \frac{D^{n'} V^{2-n'} \rho}{8^{n'-1} K \left(\frac{3n'+1}{4n'}\right)^{n'}} \qquad (4.22)$$

However, the selection of a Reynolds number of 2100 as the transition value has been criticized by numerous authors. Dodge and Metzner (1959) have indicated that the value is a function of n′ and of temperature. Ryan and Johnson (1959) introduced a more useful definition of a transition criterion, which was subsequently modified by Hanks and Christiansen (1962) and Hanks (1963), to enable the criterion to be applied to power law pseudoplastics. This criterion is a function of n′ only and is thus independent of temperature.

$$Re_c = \frac{6464n'}{(1+3n)^2\left(\frac{1}{2+n'}\right)^{\frac{2+n'}{1+n'}}} \qquad (4.23)$$

The use of Equation 4.23 as a transition criterion in this model has certain advantages over the more conventional criterion of comparing the Reynolds number to 2100. The value can be determined with reasonable accuracy and can be assumed to remain constant, provided the drilling fluid properties remain unchanged.

Different relationships are required to determine the frictional pressure losses in the drill pipe, drill bit and annulus, due to their different flow behaviour and geometry.

4.6.1 Drill String

Central to any calculation of pressure drop within a pipe is the determination of the Fanning friction factor. In the case of a drill pipe, this is complicated by the fact that the interior wall is rough, to a varying degree. Unfortunately, virtually no experimental or theoretical work has been done on the subject of non-Newtonian flow in rough pipes and either Newtonian concepts have been used or the pipe is considered smooth. If the former is assumed, an estimate of the roughness height is required.

Whereas a number of equations exist in the literature

to determine the Fanning friction factor for the turbulent flow of power law fluids in a smooth pipe, Torrance (1963) has developed the only one applicable to rough pipes. However, its origin is purely theoretical and no experimental work has been done to verify it. This equation

$$\frac{1}{\sqrt{f}} = \frac{4.07}{n'} \log \frac{r}{\varepsilon} + 6.0 - \frac{2.65}{n'} \qquad (4.24)$$

is of similar form to the familiar Nikuradse and von Kármán equations for Newtonian fluids. The one problem with this equation is that it requires a value for the roughness height which, for something like rusty commercial steel pipe, would vary enormously and be very difficult to evaluate. Fig. 4-6 indicates that for moderately pseudoplastic fluids ($n > 0.7$) the variations in the friction factor, calculated by Torrance's equation, with the roughness height is small and well within the accuracy of the other flow parameters. Hence, the roughness height itself is not a critical parameter and an average value would suffice. Usually a roughness height of 0.0006 inches is used for pipe flow calculations, although this figure is suspect for old pipe. However, on the basis of Fig. 4-6. for moderately pseudoplastic fluids, this figure would be satisfactory.

If the laminar sub-layer is of sufficient thickness then the assumption of smooth walls is valid. Dodge and Metzner (1959) derived an equation for the friction factor

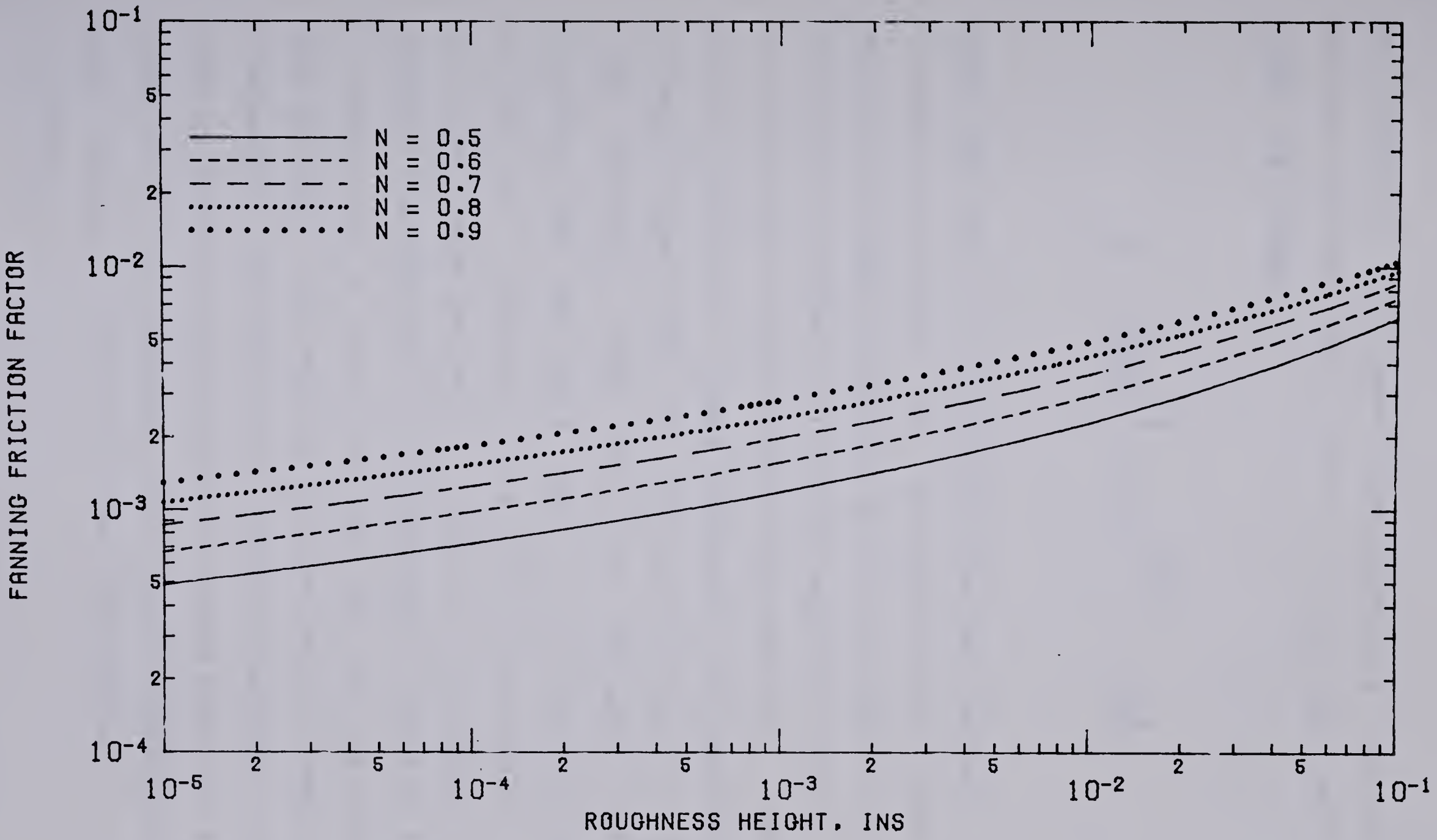


FIG. 4-6: VARIATION IN F WITH ROUGHNESS HEIGHT FOR PIPE RADIUS OF 3 INS.

as a function of the generalized parameters first used by Metzner and Reed (1959), which is directly applicable to power law fluids.

$$\frac{1}{\sqrt{f}} = \frac{4.0}{n'^{0.75}} \left[\log Re(f)^{\frac{2-n'}{n'}} \right] - \frac{0.4}{n'^{1.2}} \qquad (4.25)$$

Since then various relationships have been derived, including one by Chen (1961) who modified the original equation of Dodge and Metzner so as to be explicit in f. Solutions of a number of different equations for the friction factor in smooth pipes are summarized in Table 4-5, with the theoretical values compared to the experimental values of Bogue (1960). The relationships used are those of Dodge and Metzner (1959), Chen (1961), Mohammed (1975), Torrance (1963) and Tomita (1961), all of which are readily solvable for f. Hanks and Ricks (1975) have recently criticized Dodge and Metzner's equation and propose what is probably the best means of determining the friction factor in smooth pipe in view of the fact that only the value of n' need be known, thus ensuring that the value is temperature independent. Unfortunately the method of solution is rather laborious and more appropriate for design purposes. Whereas Table 4-5 is far from being statistically conclusive, it does indicate the validity of the Dodge-Metzner relationship.

TABLE 4.5: COMPARISON OF FANNING FRICTION FACTOR EQUATIONS FOR TURBULENT FLOW IN SMOOTH PIPES WITH THE EXPERIMENTAL VALUES OF BOGUE.

(1) Bogue (1960)
(2) Dodge and Metzner (1959)
(3) Chen (1961)
(4) Mohammed (1975)
(5) Torrance (1963)
(6) Tomita (1961)

		FANNING FRICTION FACTORS					
n′	Re	(1)	(2)	(3)	(4)	(5)	(6)
.895	98830	0.00414	0.00414	0.00400	0.00372	0.00391	0.00448
.700	12137	0.00547	0.00580	0.00587	0.00486	0.00540	0.00717
.445	12137	0.00475	0.00477	0.00482	0.00371	0.00402	0.00767
.530	17374	0.00449	0.00430	0.00439	0.00349	0.00364	0.00642
.465	12238	0.00435	0.00435	0.00444	0.00340	0.00363	0.00695
.827	31473	0.00507	0.00508	0.00509	0.00438	0.00481	0.00574
.677	8873	0.00619	0.00620	0.00626	0.00503	0.00580	0.00778

The determination of the pressure drop is readily achieved from the Fanning friction factor by means of Equation (4.26).

$$\Delta P = \frac{2f\rho V^2 L}{Dg_c} \qquad (4.26)$$

In the unlikely event that flow is laminar, the standard pressure drop - friction factor relationship would be utilized.

$$f = \frac{16}{Re} \qquad (4.27)$$

Of these various relationships, Torrance's equation for the friction factor of rough pipes (Equation 4.24) is the most suitable, with a roughness height of 0.0006 inches, in view of the fact that it is simple, allows for roughness and is independent of temperature.

4.6.2 Drill Bit

Because of the intricacy of the flow behaviour through the drill bit, the methods used to determine the fluid velocity and pressure drop through the bit have been simplified. An Equation for determining the pressure drop through the drill bit can be derived from the Bernoulli equation for flow through an orifice. Since the drill pipe cross-sectional area is very much larger than the nozzle area, the orifice coefficient is assumed to equal the

discharge coefficient. The value for the discharge coefficient is assumed to be 0.95 by Schuh (1964).

$$\Delta P_b = \frac{\rho}{2g} \left(\frac{q}{0.95An}\right)^2 \qquad (4.28)$$

4.6.3 Annulus

The annulus region is complicated by a number of factors not relevant to flow in the drill pipe, namely the volume of rock cuttings present, a factor that is often ignored in drilling hydraulics studies. Additional complications are the varying annular size (Fig. 4-1) which is often considered uniform, and the eccentricity of the rotating pipe. In a deep well on land with all the casing landed at the surface i.e. no liners present, the assumption of uniform annular size is a reasonably valid one. It becomes more questionable where a long bottomhole assembly is used, a liner is present or in offshore wells, where the riser and choke line are a complicating factor.

A number of methods exist in the literature for incorporating the eccentricity of a rotating pipe into annular flow equations. However, all assume that the eccentricity is regular and the degree of eccentricity is known. Neither applies to this particular case and the irregularity of the eccentricity necessitates that it be neglected with regard to the derivation of the relevant flow equations.

As mentioned above, the flow behaviour in the annulus should ideally be laminar and this is normally the case. However, as with pipe flow, Hanks' stability criterion (Equation 4.23) can be applied to confirm that this is the case in each section of the annulus. The fact that the flow should be laminar removes the significance of the rough surfaces (Bowen 1961), so the pressure drop can be determined by means of a smooth walled annular flow equation of which a number exist.

The original work in this field was that of Fredrickson and Bird (1958) which is still considered the most accurate method of determining annulus pressure losses. Unfortunately the exact solution for power law fluids in an annulus is intricate unless use is made of graphs. For this reason several attempts have been made to simplify the procedure or to derive the solution by different means. One common way was to modify pipe flow equations by means of the hydraulic radius concept and although this resulted in simple equations the validity of this concept has been subjected to a great deal of criticism. Another more accurate, and less controversial method, involved approximating the annulus by two parallel plates. A number of the most applicable methods are compared with the Fredrickson and Bird method in Table 4-6 by solving each using example data from Skelland (1967). As with pipe flow equations this table is far from conclusive but it does indicate that any of the methods are

TABLE 4.6: COMPARISON OF PRESSURE DROPS OBTAINED USING VARIOUS ANNULAR FLOW EQUATIONS TO CALCULATE THE PRESSURE GRADIENT USING AN EXAMPLE IN SKELLAND (1967), PAGE 115.

(1) Fredrickson and Bird (1958).....60.85 lb/ft²/ft

(2) Fredrickson and Bird (Parallel Plate)..61.50 lb/ft²/ft

(3) Fredrickson and Bird (Annular Slit)....54.90 lb/ft²/ft

(4) Savins (1958).....61.20 lb/ft²/ft

(5) Mishra and Mishra (1976).....60.69 lb/ft²/ft

(6) Wallick and Savins (1969).....60.75 lb/ft²/ft

applicable. [1] However, those of Savins (1958) or the parallel plate approximation of Fredrickson and Bird (1958) are the easiest to apply, the remainder involving the use of iterative or numerical methods of solution. It is the parallel plate approximation of Fredrickson and Bird (1958) that is used in this study in view of the fact that the geometry of the system being modeled is such that the parallel plate approximation is valid for the annulus. (Equation 4.29)

$$\Delta P_a = \frac{2KL}{(r_o - r_a)g_c}\left[\frac{2(n'+1)q}{\pi n'(r_o + r_a)(r_o - r_a)^2}\right]^{n'} \qquad (4.29)$$

Thus, the frictional pressure losses may be determined for the drill string, drill bit and annulus using equations 4.26, 4.28 and 4.29, respectively. The sum of these frictional pressure losses should equal the pump circulating pressure less the frictional pressure losses in the surface connections. From the pump circulating pressure, flow rate and mechanical efficiency, the input horsepower is calculated by Equation 4.30 and divided between the drill string, drill bit and annulus by the ratios of their respective frictional pressure losses.

$$HP = \frac{\Delta Pqe}{1.98 \times 10^6} \qquad (4.30)$$

[1] The annular flow equation derived by Mishra and Mishra contains a typing error which has been allowed for in Table 4-6. Skelland's solution is wrong and has been corrected by Mishra and Mishra.

These values are converted from thermal to mechanical energy by Equation 4.31,

$$E = 2544.9\ HP \tag{4.31}$$

and added to the energy values already determined for the work done at the drill bit and the work required to rotate the drill string.

The resulting values are the energy source terms used in the model.

5. DISCUSSION OF RESULTS

Once the computer model had been designed and made operational, it was used to simulate wellbore temperature distributions under a variety of conditions. Two versions of the computer program were used, namely;

1. A "full scale" model incorporating a full well completion of up to three casing strings and using the data in Table 4-1 to give a reference temperature distribution.
2. A "simplified" model which neglected the well completion and assumed a uniform hydraulic radius with neither casing nor cement present. The relevant data in Table 4-1 were also used by this model to produce a second reference temperature distribution.

The annulus temperature profiles for the two different versions are shown in Fig. 5-1.

5.1 Comparison with Previous Models

It is not possible to compare the annulus temperature profiles generated by this model, with those for most previous models because the respective authors have not included sufficient data. Often values are not given for parameters which are shown later in this chapter to be very significant, e.g. Raymond (1969) includes all data except the fluid heat capacity, which is shown to be the most

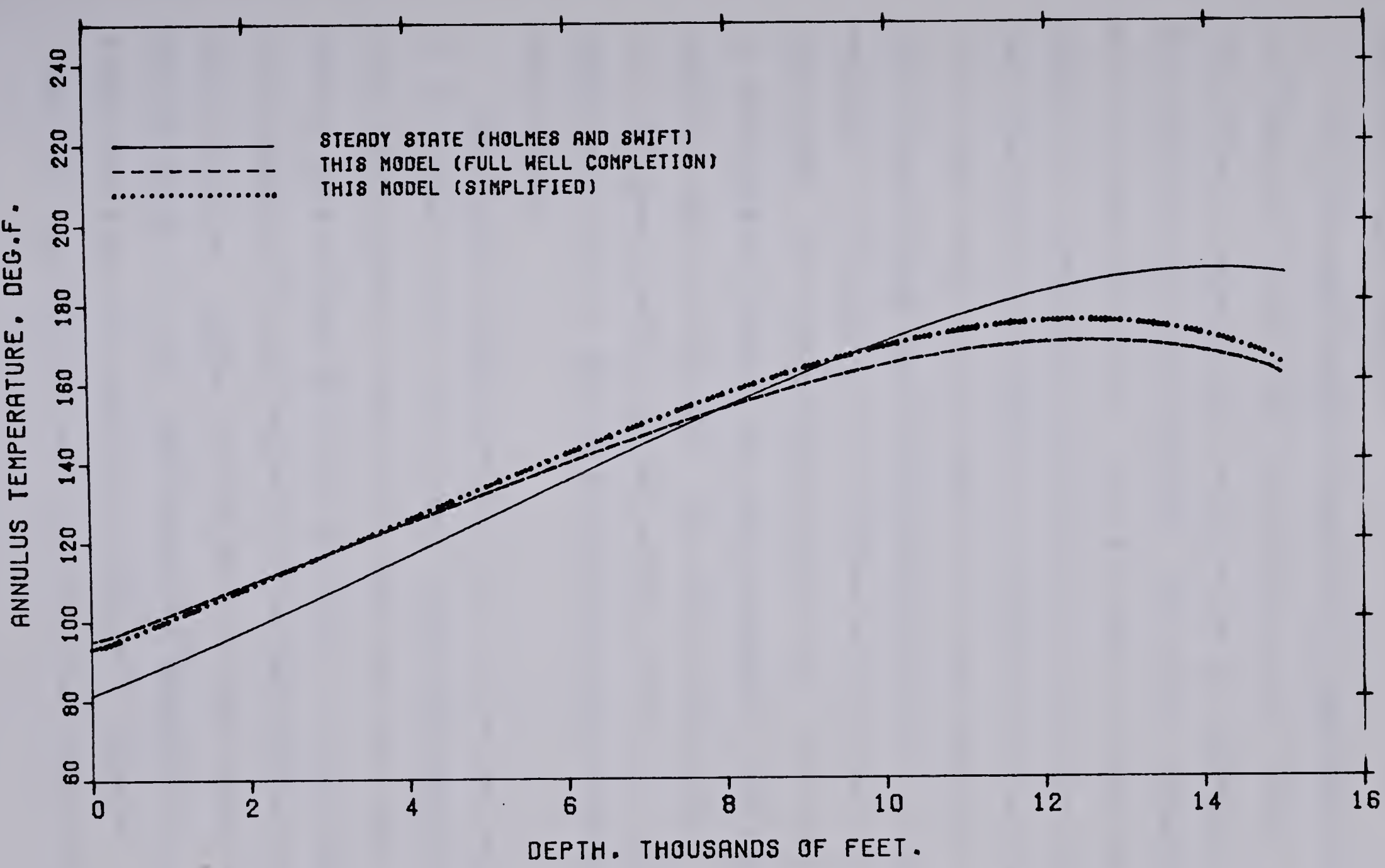


FIG.5-1: COMPARISON OF ANNULUS TEMPERATURE PROFILES

significant parameter of all in terms of its influence on the temperature profile.

The only models which allow direct comparison are those of Holmes and Swift (1970) and Keller et al. (1973). Since this model is essentially the Keller et al. model but with a much improved solution procedure, the annulus temperature profiles are very similar. Fig. 5-1 shows a comparison between the temperature profile of Holmes and Swift and the two versions of this model. It is evident that the steady state model of Holmes and Swift is in poor agreement with the unsteady state model developed by Keller et al. and extended in this work. It is further evident that the added improvement, of considering casing strings and alterations in the hydraulic radius, has only a marginal effect on the annulus temperature profile. The annulus temperature profiles generated by the two versions differ by a maximum temperature of 5°F, and the bottomhole temperatures are almost equal.

The annulus temperature profiles for the two versions of this model in Fig. 5-1 do not include heat generation within the system in view of the fact that the energy sources were ignored by Holmes and Swift. If heat generation is included in the two unsteady state temperature profiles, as Keller et al. appear to have done in their comparison (Keller et al. Fig. 2), the bottomhole temperatures are almost identical for the data in Table 4-1. However, in this study (see Fig. 5-1) it was found that the Holmes and Swift

annulus temperature profile continuously diverges from the unsteady state temperature profile up the annulus, and the outlet temperatures differ by about 20°F. This contradicts Keller et al. Fig. 2 in their work indicates similar outlet temperatures for the unsteady state temperature profile and the Holmes and Swift temperature profile. Whether energy sources are included or not, agreement between the steady state Holmes and Swift annulus temperature profile and the unsteady state annulus temperature profiles of this model is very poor. This is not altogether surprising considering that Holmes and Swift used different and simpler equations to describe the wellbore heat flow, and consequently were able to use an analytical solution.

It should be noted that where a long string of drill collars is present, this must be allowed for in calculating the frictional pressure losses for the drill string and annulus in the "simplified" model. Large errors may occur in the respective energy source terms if only the drill pipe were considered.

The effects of considering the energy sources in the system are shown in Fig. 5-2 and agree closely with a similar graph in the paper of Keller et al. Fig. 5-2 confirms the necessity of including energy sources in any model that attempts to estimate such temperature distributions, in view of the fact that there is an error of about 30°F in the bottomhole temperature when heat generation is ignored.

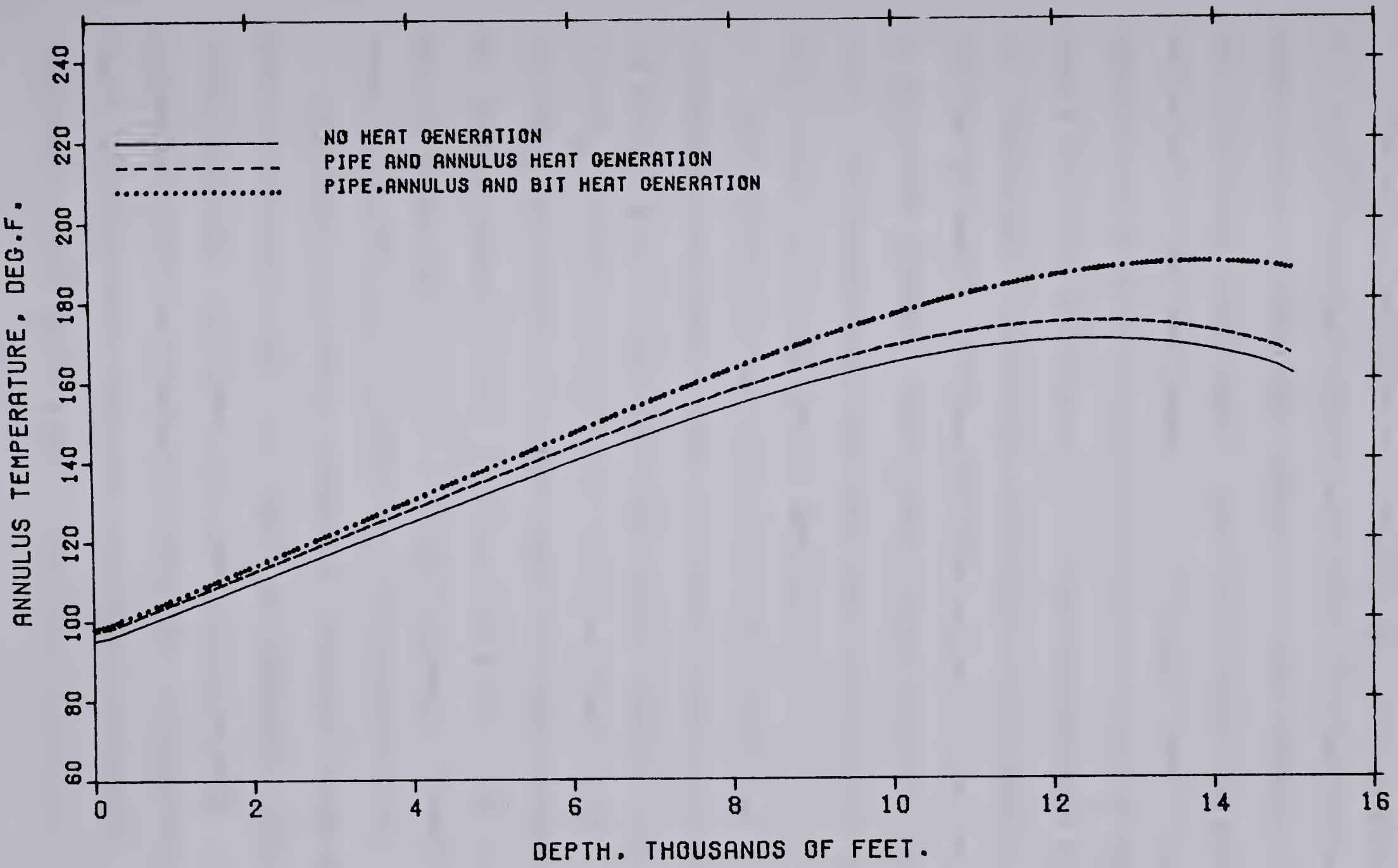


FIG.5-2: EFFECT OF HEAT GENERATION ON THE ANNULUS TEMPERATURE PROFILE.

5.2 Parametric Sensitivity Analysis

The major advantage in carrying out such an analysis is to ascertain to what extent variations in a particular parameter will affect the temperature distribution in the wellbore. This is of special importance where the particular parameter is one that cannot be evaluated directly, and instead must be given an assumed value. In such a case, the degree to which variations in this parameter would affect the temperature indicate how important is an accurate value for the parameter. It also provides a qualitative estimate of the error inherent in the model caused by using assumed values. Such parameters would be those relating to the earth, such as the geothermal gradient.

Some parameters which have a strong influence on the temperature distribution can be directly and accurately evaluated, e.g. circulating time, depth, geometry and drilling fluid characteristics. Such an analysis is therefore less important with regard to these parameters, but nonetheless pertinent in view of the fact that it can be used to judge the validity of assuming some of them to remain constant e.g. the drilling fluid properties.

Any model of such an imprecise and complicated an operation as drilling a well must, by necessity, be a simplification. The fewer the simplifications and assumptions, the more accurate the model. Unfortunately, there is no physical means of measuring the dynamic temperature profile in a well, and hence there is no

independent way of assessing the accuracy of the model. For this reason, any variation in a parameter that caused a maximum deviation in the annulus temperature profile of less than 5°F was considered insignificant. It should be noted that interaction between parameters was ignored and that if several of the parameters were varied simultaneously, it is possible that, whereas individually such variation had an insignificant effect, the sum effect could be significant.

With regard to the actual design of the computer program, the following observations were made.

1. The use of double precision arithmetic instead of single precision, had no effect on the resulting annulus temperature profiles, thus permitting a 100% reduction in the computer memory storage requirements.
2. The number of time steps used had no effect on the solution, which is to be expected from a direct, implicit solution method.
3. The size and number of the vertical elements in the matrix had an insignificant effect on the annulus temperature profile for a 15,000 feet well as long as the elements were less than 500 feet in size. It was observed that, in general, the vertical element size had to be less than 3% of the total well depth to ensure that the annulus temperature profile remained independent of the vertical element size.
4. The optimum size and number of the radial elements in the matrix was more difficult to assess. If the radius

of the external radial boundary is too small then there will be heat buildup along this boundary because of the external radial boundary condition, which prohibits the flow of heat across the boundary into the surrounding formation. Long circulation times or excessive heat generation will cause the radial temperature gradient to intersect the external boundary before the gradient has achieved a constant temperature. Ten radial elements were arbitrarily used by Keller et al. (1973), of which the first seven were spaced in such a way as to represent the various individual sections of the wellbore (Fig. 4-2) and the remaining three used to represent the earth. The same arrangement was used in this work with the three outer radial elements being each two feet wide, so as to satisfy the external radial boundary condition. Varying the size of these three outer elements within one order of magnitude had no significant effect on the annulus temperature profile provided there was no heat buildup along the boundary. However, with the simplified version of the model the radial element size is much more important in view of the fact that only the first three elements can be spaced to coincide with the physical dimensions of the pipe and annulus. Reducing the number of radial elements had an adverse effect on the annulus temperature profile, as did alterations in their size. If the seven outer elements are all of the same size, the optimum

size is the minimum to satisfy the external radial boundary condition for a given circulation time. Unfortunately, increasing the circulation time will cause a heat buildup along the boundary and consequently create discrepancies in the annulus temperature profile. This situation was avoided by reducing the size of the fourth to seventh elements and fixing the size of the three outermost elements at 2 feet each. This closely approximates the real case where casing strings are present. It was found that the closest agreement between the two versions was achieved when the fourth to seventh elements were each 0.5 feet in width and the three outer elements were each two feet in width. Not only was the annulus temperature profile insensitive to changes in the element size for this case, but no heat buildup occurred along the external boundary, irrespective of the circulation time.

5. The steady state model of Holmes and Swift has already been shown to be inadequate. A more meaningful comparison of steady state and unsteady state annulus temperature profiles is achieved in Fig. 5-3 where an assumed steady state annulus temperature profile was generated by solving the model for a circulation time of 1,000 hours. Not only is this profile completely different from that of Holmes and Swift, but it further supports the contention that the steady state approximation of wellbore heat transfer is not

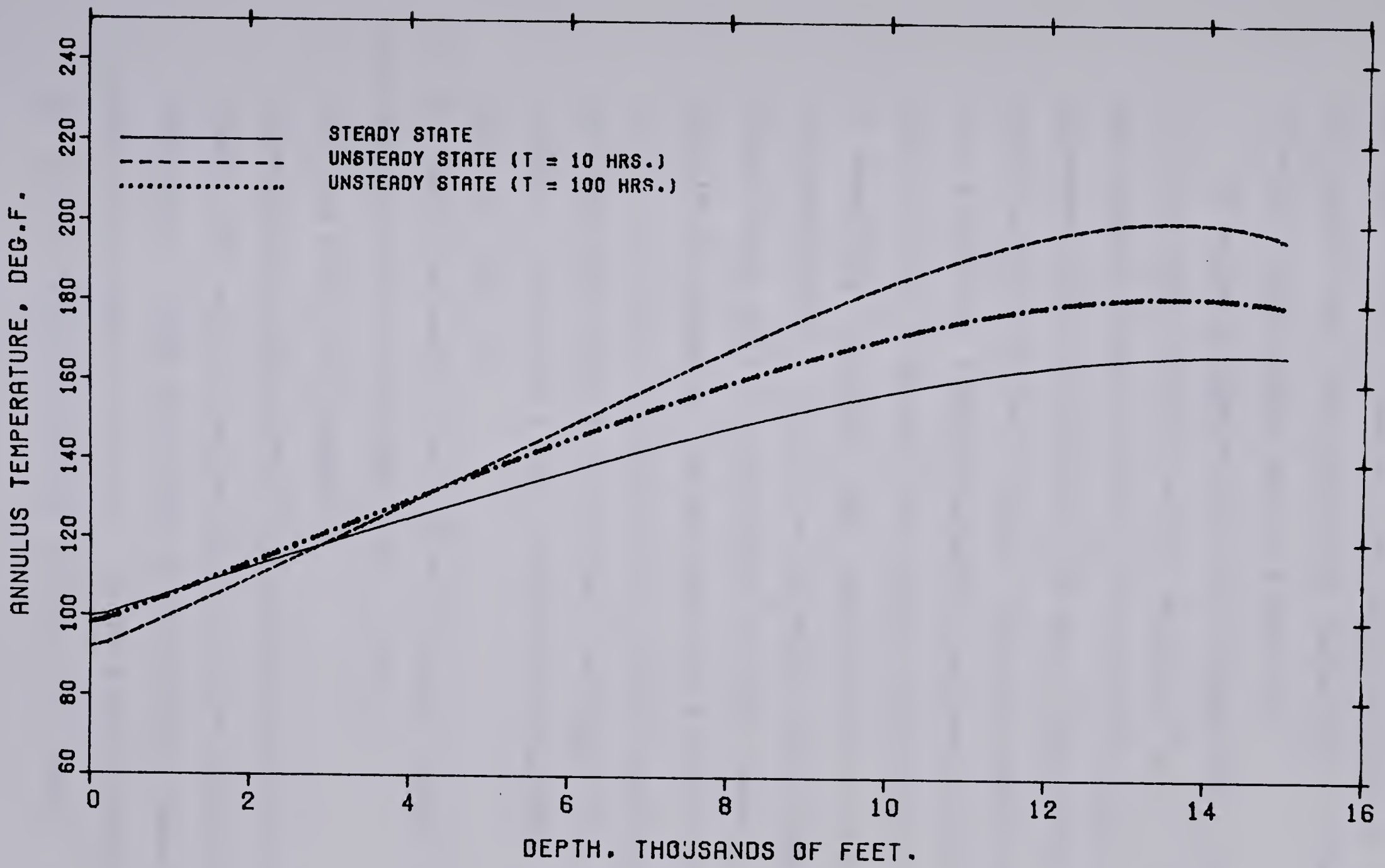


FIG.5-3: COMPARISON OF THE STEADY STATE AND UNSTEADY STATE ANNULUS TEMPERATURE PROFILES.

justified. Even after circulating for 100 hours, the maximum feasible time of continuous circulation likely for any bit run, the bottomhole temperature differed from the steady state one by almost 20°F.

An anomaly appears to exist between Fig. 2 and Fig. 3 in the work of Keller et al. Whereas Fig. 3 in their work agrees closely with Fig. 5-3 in this study, no agreement exists between the 24 hour temperature profiles in their two figures. The data used to generate Fig. 2 and Fig. 3 are presumably the same so the 24 hour curve in Fig. 2 should match one of the curves in Fig. 3, depending on whether heat generation was included in the generation of Fig. 2. No agreement exists and insufficient detail is included in their paper to explain the anomaly. The unsteady state profiles shown in Fig. 2 of Keller's paper could not be reproduced by the model developed in this study, although the curves in Fig. 3 of Keller's paper could be reproduced, as shown in Fig. 5-3.

The following parameters were found to have a significant influence on the annulus temperature profile.

1. Drilling fluid heat capacity

 Increasing or decreasing this parameter by 50%, which covers the range of values quoted in the literature, resulted in large variations in the annulus temperature profile as shown in Fig. 5-4. Since a small change in the value of this parameter results in a large

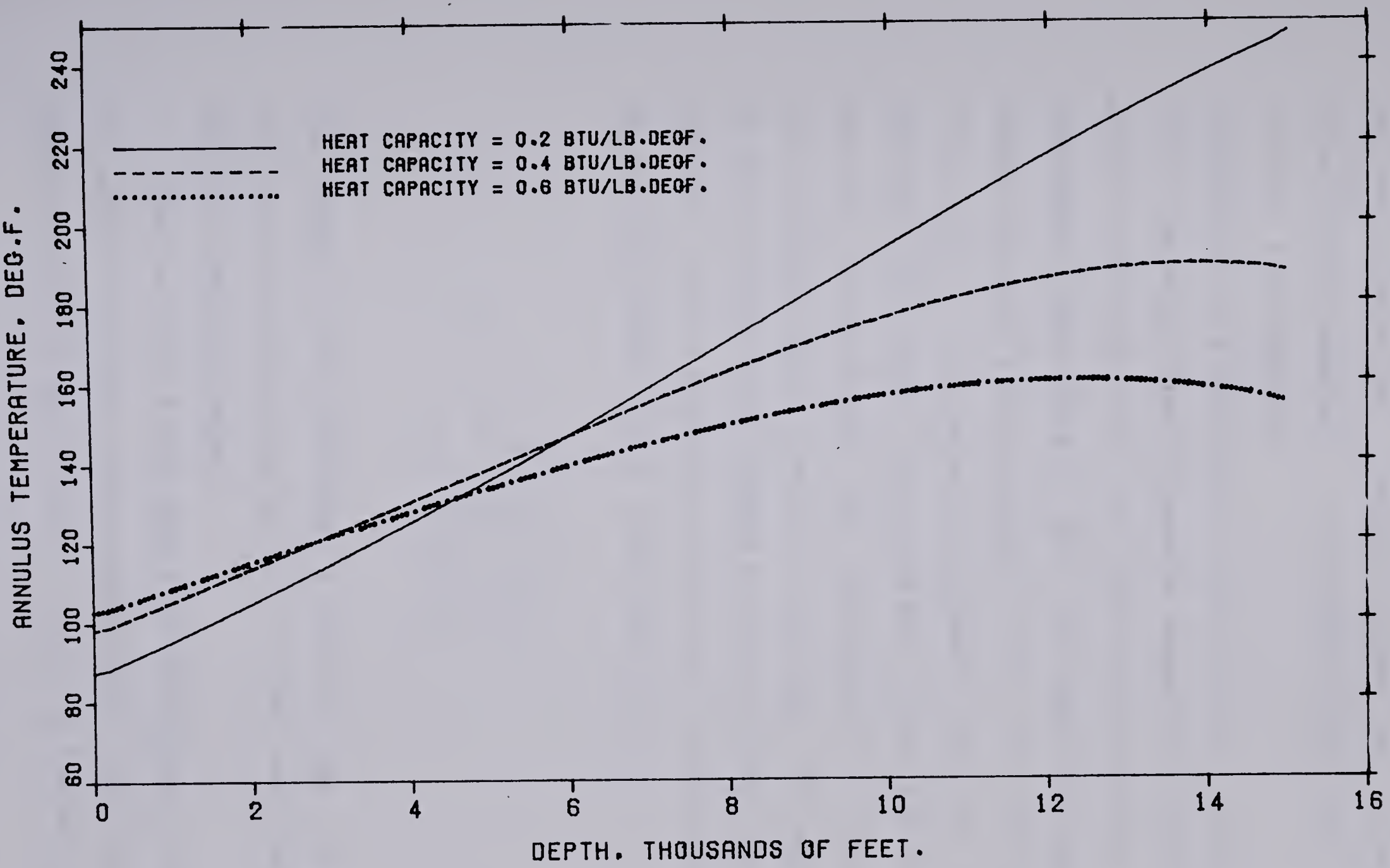


FIG.5-4: EFFECT OF VARIATIONS IN THE MUD HEAT CAPACITY ON THE ANNULUS TEMPERATURE PROFILE.

alteration in the annulus temperature profile, and as the variation of this parameter within the system cannot be accurately assessed, it is highly significant.

2. Drilling fluid density

Increasing the fluid density from 75 lb/ft^3 to 100 lb/ft^3 decreased the bottomhole temperature by 22°F, whilst increasing it to 120 lb/ft^3 decreased the bottomhole temperature by 38°F. The resulting annulus temperature profiles are shown in Fig. 5-5. Although the fluid density is known with reasonable accuracy upon entering the system, its variations within the system are not. In particular, the fluid density in the annulus will increase due to the drill cuttings. The magnitude of this increase will depend on the drilling rate, the hydraulic radius and the circulation rate and can be determined approximately from Equation 5.1.

$$\rho_a = \frac{\rho + \frac{x}{Z}\left(\frac{r_o^2}{r_o^2 - r_a^2}\right)\rho_f}{1 + \frac{x}{Z}\left(\frac{r_o^2}{r_o^2 - r_a^2}\right)} \qquad (5.1)$$

The effect of this increase is shown in Fig. 5-6 and obviously should not be ignored, as has been the case with all previous models.

The range of fluid densities considered in Figs. 5.5 and 5.6 reflects the maximum likely fluctuation in densities due to gas or water influx to the annulus or

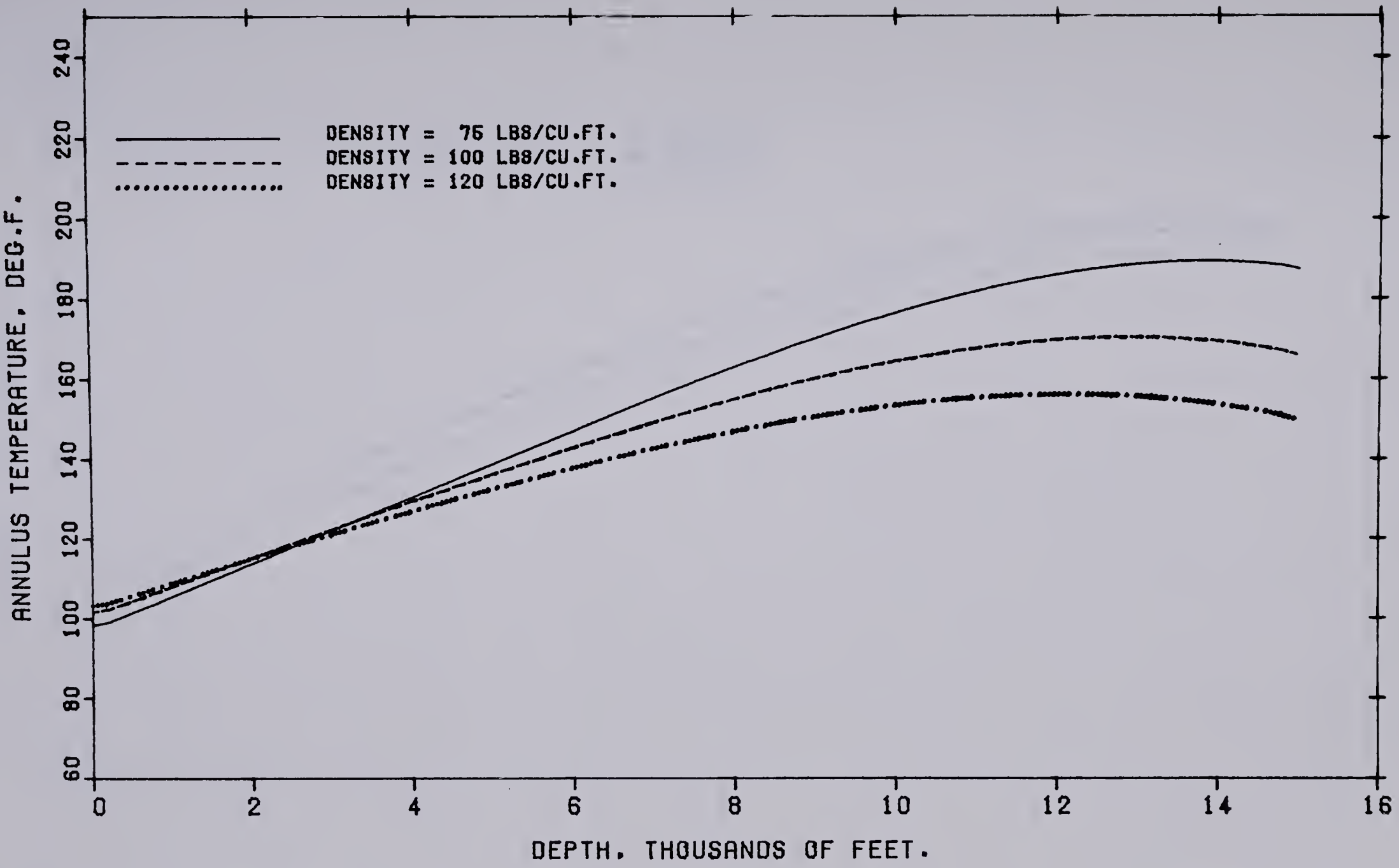


FIG.5-5: EFFECT OF VARIATIONS IN THE MUD DENSITY ON THE ANNULUS TEMPERATURE PROFILE.

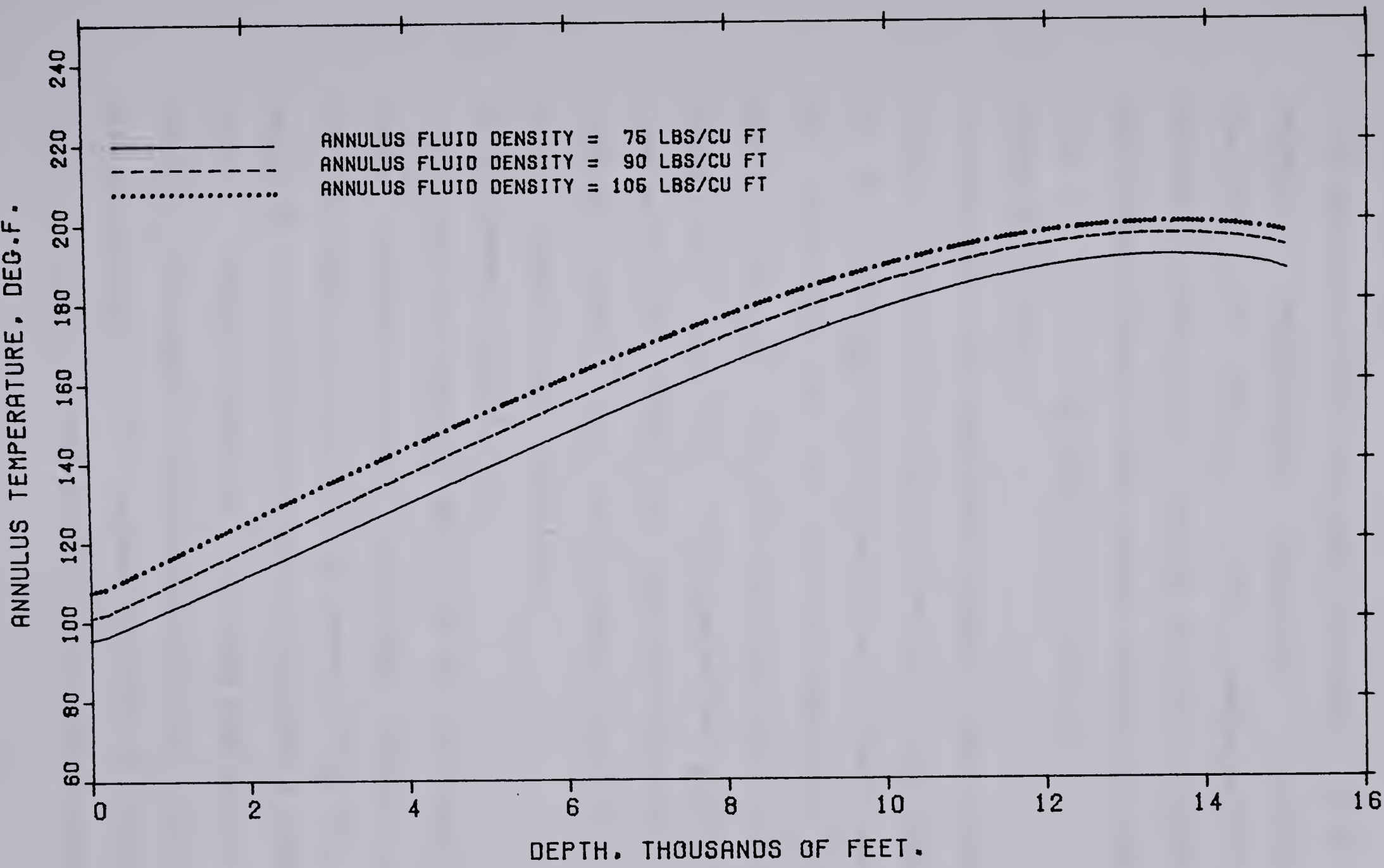


FIG.5-6: EFFECT OF ALLOWING FOR THE CUTTINGS DENSITY ON THE ANNULUS TEMPERATURE PROFILE.

drill cuttings buildup in the annulus.

3. Fluid flow rate

 A 25% decrease in the flow rate resulted in a 25 °F increase in the bottomhole temperature. Increasing the flow rate by 25% resulted in a 20°F decrease in the bottomhole temperature. Although the flow rate has a significant effect on the annulus temperature profile (Fig. 5-7) it can be accurately measured.

4. Geothermal gradient

 Alterations in the geothermal gradient have a marked effect on the annulus temperature profile as shown in Fig. 5-8. Although this parameter will remain constant for a particular well, it cannot be known with any degree of accuracy. Fig. 5-8 indicates that a poor assumption of the value of the geothermal gradient will cause errors in the annulus temperature profile. The range of values in Fig. 5-8 is representative of the values quoted in the literature.

5. Earth thermal conductivity

 A four-fold variation in the value for the earth's thermal conductivity had a significant effect on the annulus temperature profile as shown in Fig. 5-9. Reducing it by 400% decreased the bottomhole temperature by 20°F, whilst increasing it by 400% had only a slight effect on the annulus temperature profile. Although a 400% alteration in this parameter within a wellbore is highly unlikely, it represents the complete range of

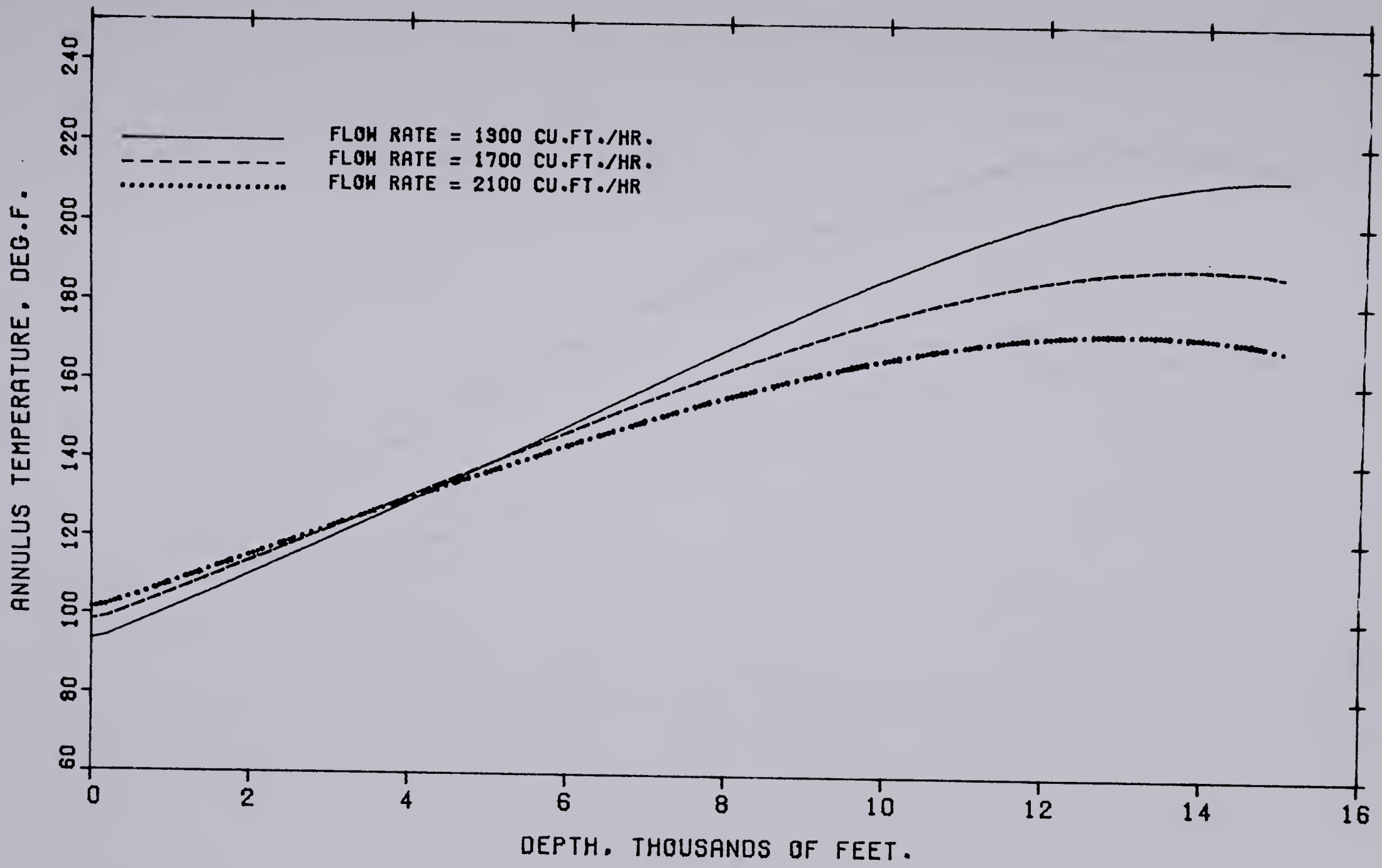


FIG.5-7: EFFECT OF VARIATIONS IN THE MUD FLOW RATE ON THE ANNULUS TEMPERATURE PROFILE.

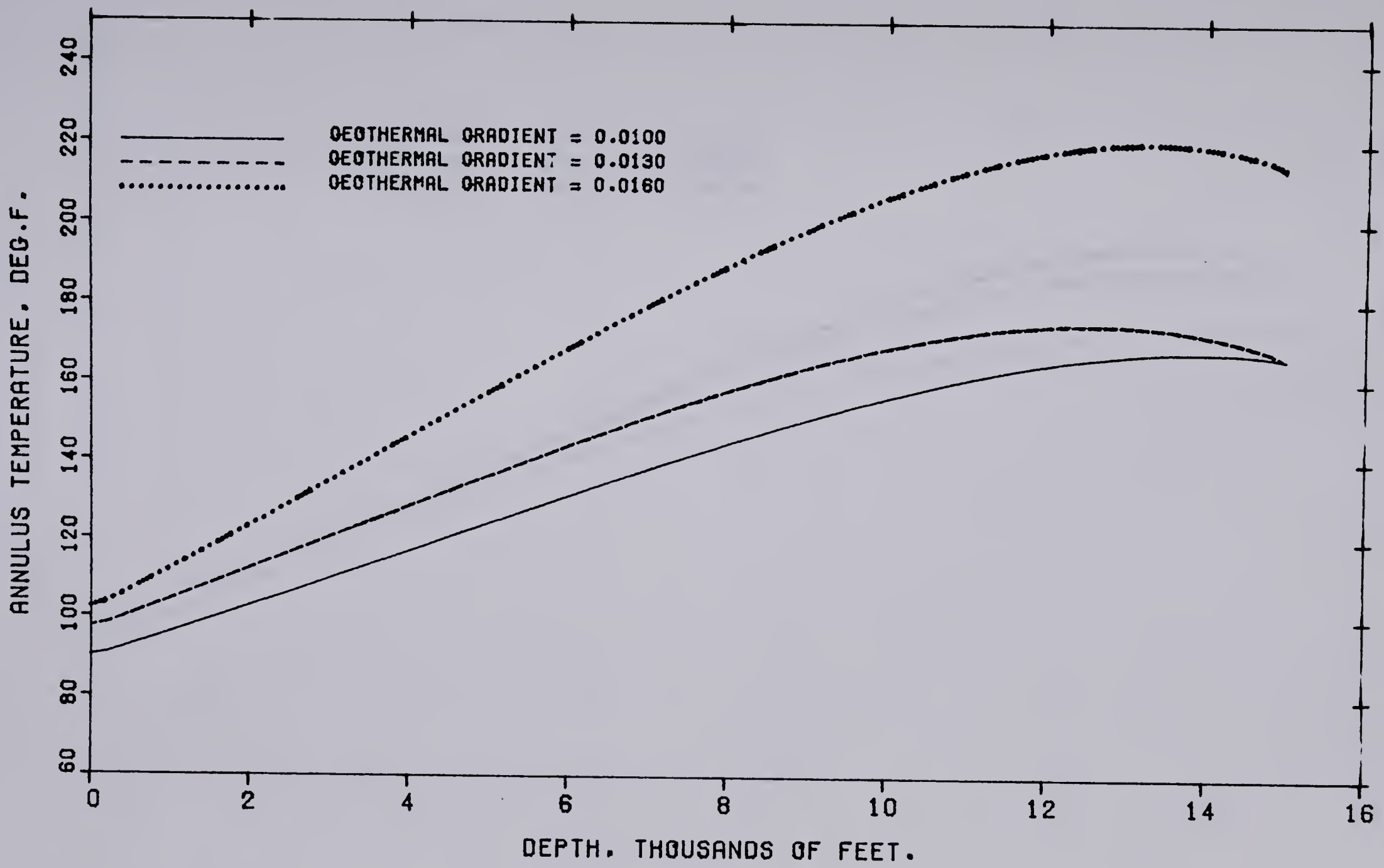


FIG.5-8: EFFECT OF VARIATIONS IN THE GEOTHERMAL GRAD. ON THE ANNULUS TEMPERATURE PROFILE.

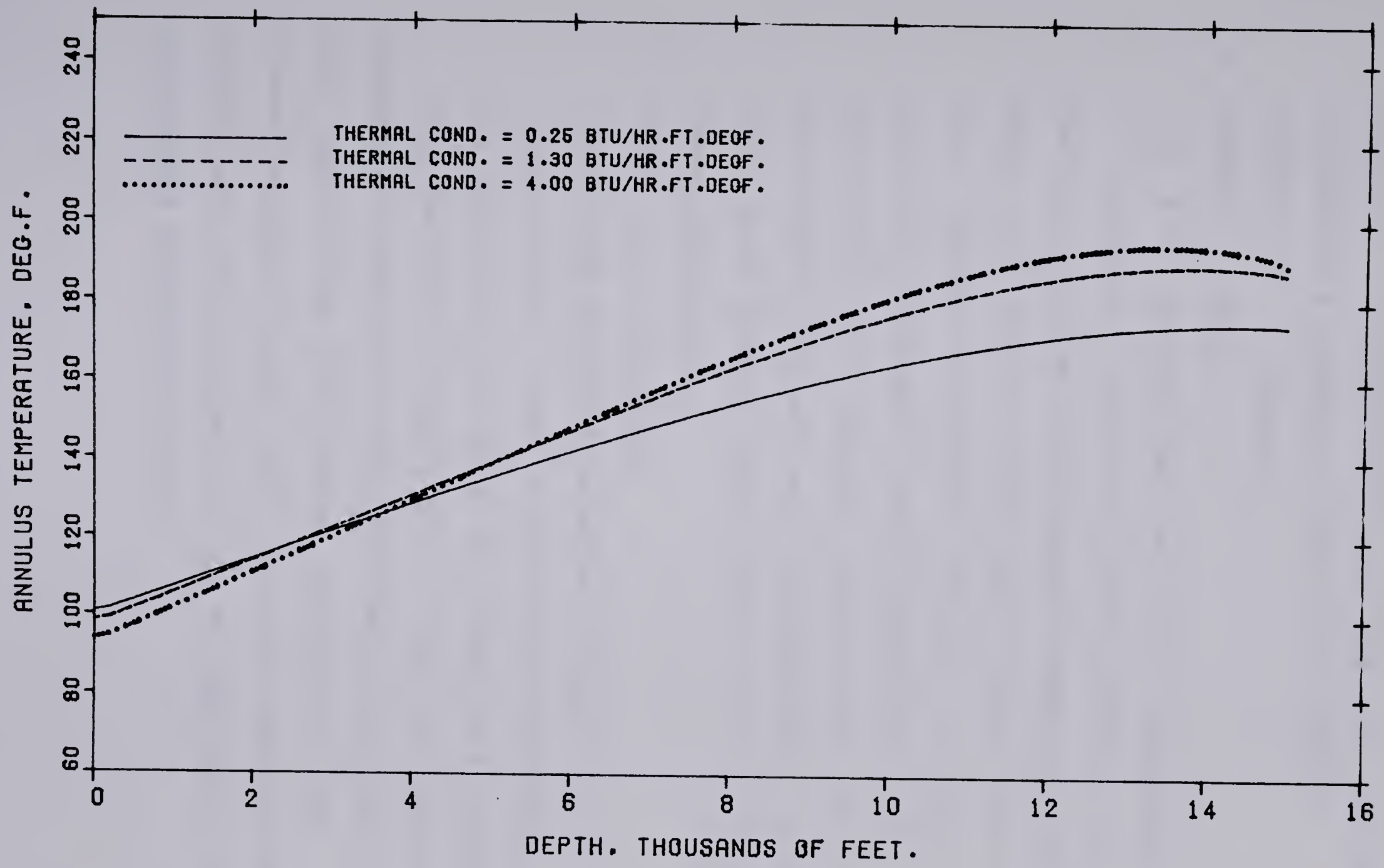


FIG.5-9: EFFECT OF VARIATIONS IN THE EARTH'S THERMAL CONDUCTIVITY ON THE TEMP. PROFILE.

possible thermal conductivities. It is a parameter that cannot be measured directly and Fig. 5-9 indicates that a reasonable estimate of the earth's thermal conductivity is required.

6. Hydraulic radius

 Fig. 5-10 indicates that the annulus temperature profile is relatively insensitive to this parameter with a maximum variation in the annulus temperature profile of about 10°F. This is further justification for the use of the "simplified" version of the model in view of the fact that it assumes a uniform hydraulic radius. The variations in the hydraulic radius in Fig. 5-9 are over the length of the well and the assumption of a constant value would involve a much smaller error in the annulus temperature profile.

7. Inlet fluid temperature

 This can be accurately measured although Fig. 5-11 indicates that it must be continuously monitored during the operation of the model at the wellsite to ensure that the annulus temperature profiles are accurate.

Reasonable variations in the earth density and specific heat, the drilling fluid thermal conductivity, the convective heat transfer coefficients and the drill pipe density and thermal properties, had no significant effect on the annulus temperature profile.

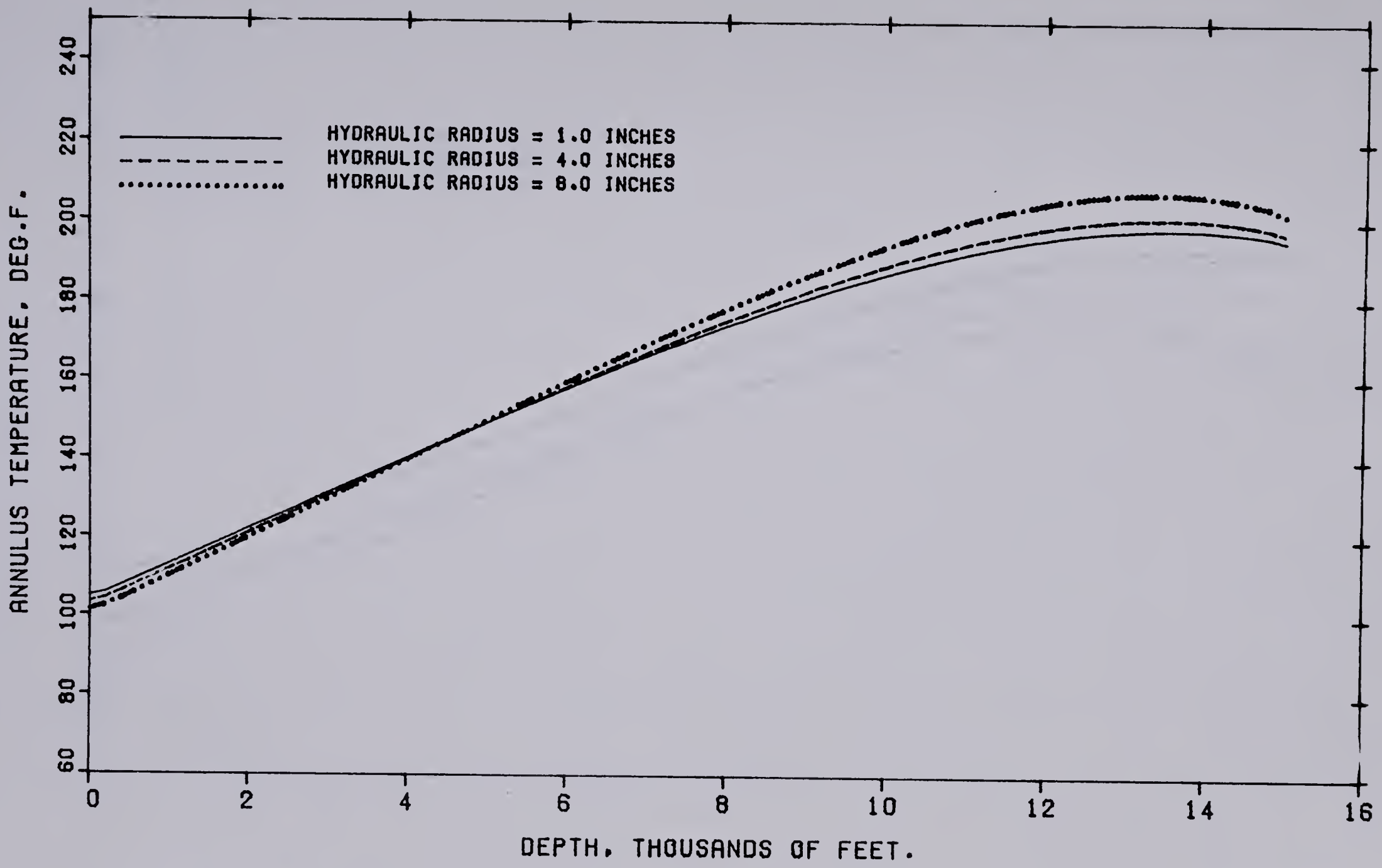


FIG.5-10: EFFECT OF VARIATIONS IN THE HYDRAULIC RADIUS ON THE ANNULUS TEMPERATURE PROFILE.

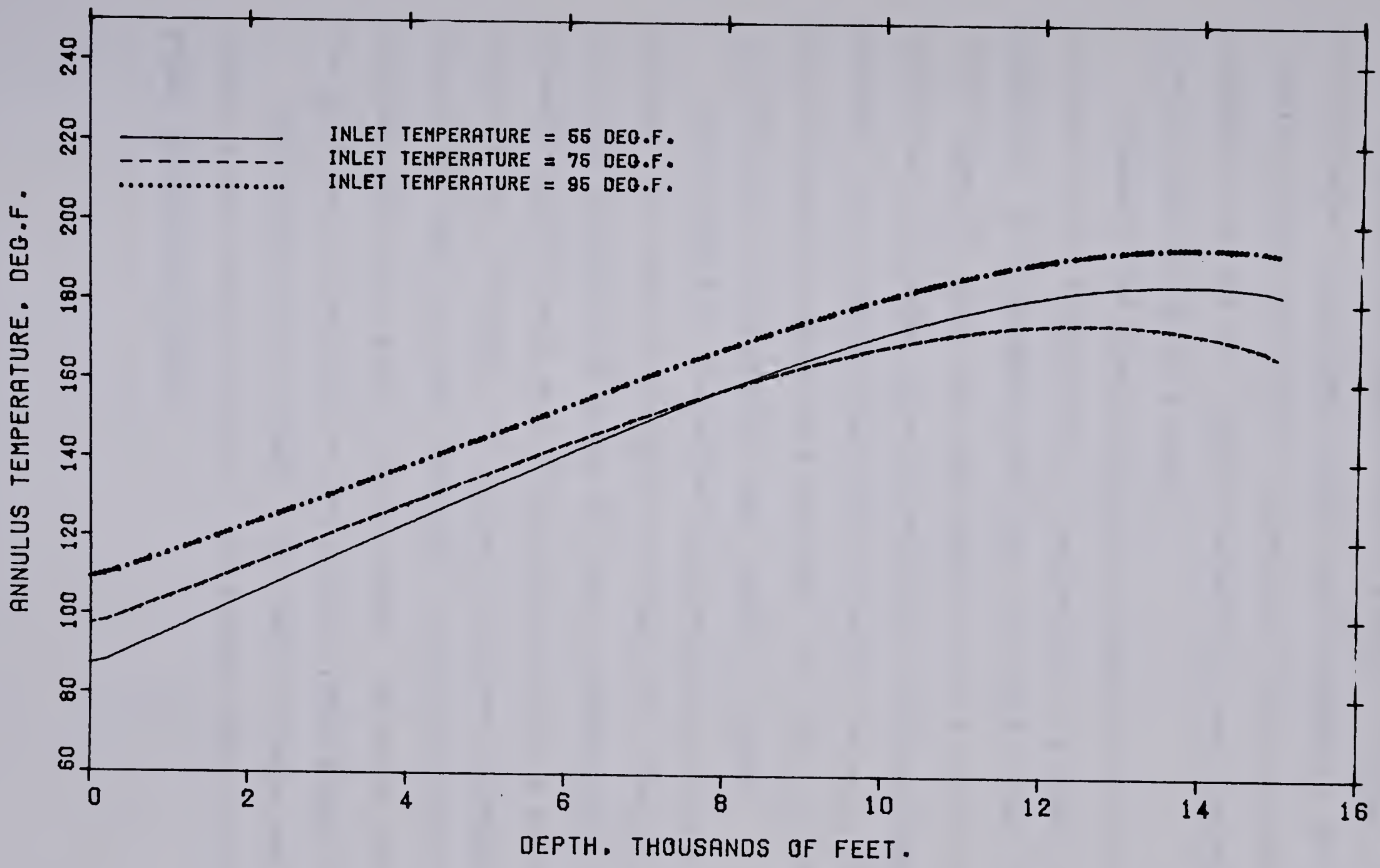


FIG.5-11: EFFECT OF VARIATIONS IN THE INLET FLUID TEMP. ON THE ANNULUS TEMPERATURE PROFILE.

5.3 Validity of the Assumptions

There is no evidence from this work to suggest that any of the major assumptions enumerated in Chapter 4 are invalid. Given the physical geometry of the system being modeled, they are all logical assumptions and the problem is greatly simplified as a result.

However, the final assumption, namely that the fluid properties are independent of temperature, is open to question. It is evident from Figs. 5.4 and 5.5 that the fluid specific heat and fluid density have a significant effect on the temperature distribution. No investigation was carried out to assess the extent to which these parameters are affected by temperature and until this is done, the validity of this assumption must remain in doubt.

With regard to the assumptions made by previous workers, the implied assumption of Newtonian flow behaviour is valid from both the point of view of convective heat transfer coefficients and the calculation of the energy source terms. Although this assumption gives increased values for the frictional pressure in the drill pipe and the annulus, and hence energy source terms, the error causes an insignificant alteration in the annulus temperature profile.

The assumption of steady state heat transfer and ignoring the energy sources in the system, have already been shown to be unjustified.

5.4 Wellsite Operation of the Model

Information on the wellbore temperature distribution is most likely to be required after the surface and conductor casing strings have been set. The operation of this model would be most suited to periods of constant drilling through thick, uniform formations, a situation most likely to occur after several thousands of feet have been drilled. Because the initial temperatures in the system are assumed to be the geothermal gradient, this will only be valid prior to the commencement of drilling when the temperature profile will not have been disturbed. Thus, for the operation of the model to begin at some point during the drilling of the well, an estimate must be made of the initial temperatures prevailing at that time.

If the operation of this computer model is assumed to commence after a casing string has been set, a logical starting point, then two options exist for determining the initial temperatures. Either the static bottomhole temperature obtained from a logging tool could be used to give a "pseudo-geothermal gradient", or if sufficient time had elapsed since the last period of circulation, the temperature distribution in the wellbore would have reverted approximately to the geothermal gradient. Fig. 5-12 indicates that the annulus temperature profile reverts almost to the geothermal gradient after about 2 days without circulation. This is about the minimum time required to run a casing string.

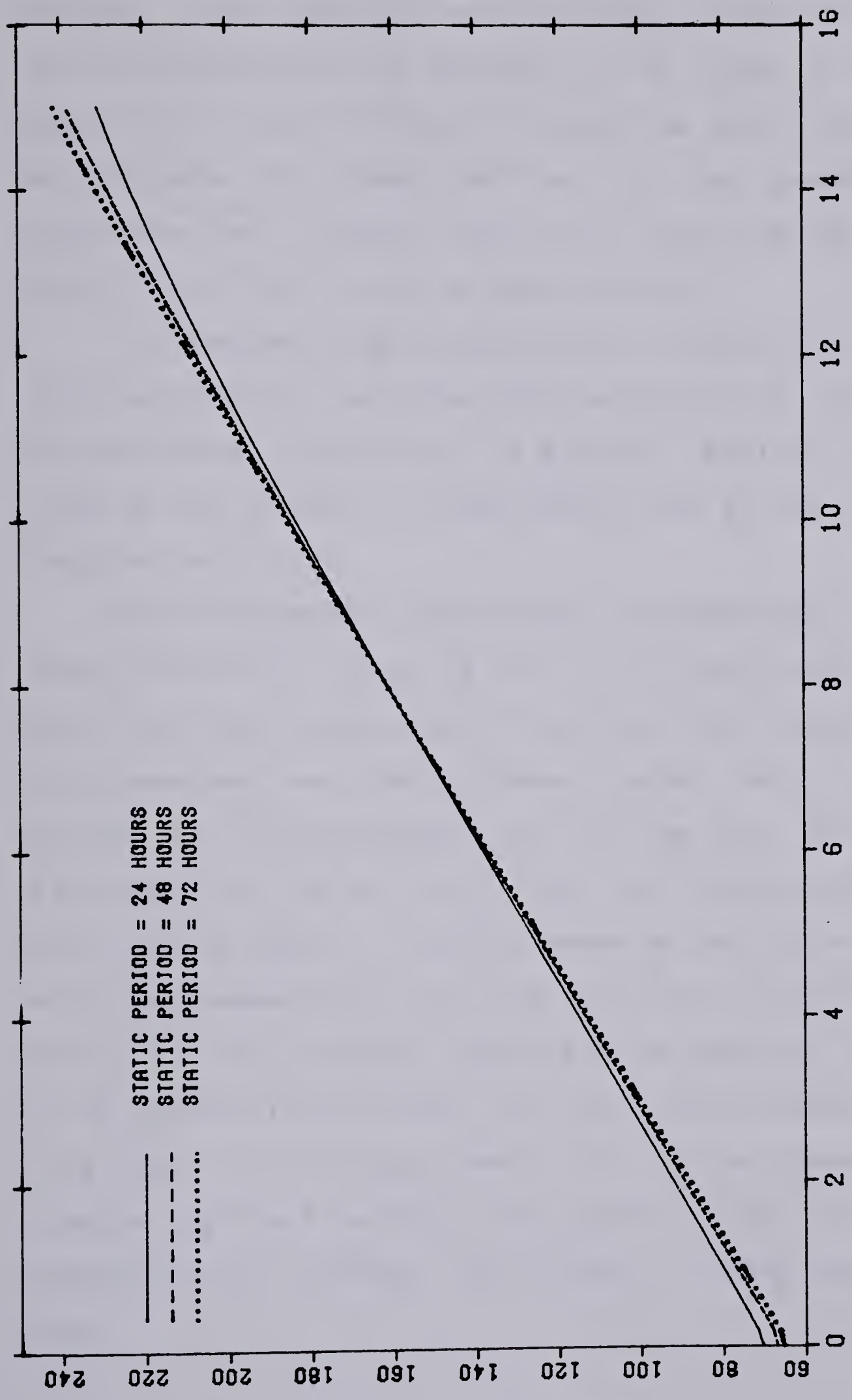


FIG.5-12: APPROXIMATION OF ANNULUS TEMPERATURE PROFILE TO INITIAL CONDITIONS AFTER 24 HRS. FLOW.

For the static case, heat transfer is by radial and vertical conduction only and convection is negligible. Thus, the third assumption in Chapter 4 is no longer valid and Equations 4.1 and 4.3 should be modified accordingly. This was not done and instead the flow rate, heat generation and convective heat transfer coefficients were reduced to zero. Hence, Fig. 5-12 is only an approximation.

The computer program should be initiated when circulation first commences after a casing run with either the geothermal gradient or the gradient obtained from a logging tool bottomhole temperature, used as the initial temperature profile.

Once the computer program has commenced generating temperature data, it may be left to run continuously, obtaining the necessary data from electronic sensors after predetermined time intervals have elapsed. Hence, the salient drilling parameters such as flow rate, drilling fluid density, and drilling fluid inlet temperature can be continuously updated. Should a means be available to accurately measure the drilling fluid heat capacity at the wellsite, this parameter should also be updated. In fact it is an essential requirement for the accurate operation of this model. If drilling ceases, this can be allowed for by considering the flow rate, heat generation and the convective heat transfer coefficients as being equal to zero.

6. SUMMARY AND CONCLUSIONS

The primary objective of this work was to develop a computer model that estimates the temperature distribution in a wellbore both accurately and quickly. This model was then used to examine the validity of the assumptions made in this and previous models, and to investigate the significance of the parameters in terms of their effect on the temperature distribution. The results of this investigation contradicted, in several instances, conclusions reached by previous workers.

The major conclusions of this study are as follows:

1. Using a band algorithm, direct solution technique to solve the finite difference equations describing the transient heat flow in a wellbore, a solution time of about 3 seconds was required on the University of Alberta's Amdahl 470 computer as compared to 170 seconds on a CDC 6400 quoted by Keller et al. (1973). The Amdahl 470 is approximately five times faster than the CDC 6400, so the solution method used in this work is an order of magnitude faster than the method used by Keller et al.
2. The following parameters have a significant effect on the wellbore temperature distribution.
 a. drilling fluid heat capacity
 b. drilling fluid density
 c. drilling fluid flow rate

d. drilling fluid inlet temperature

e. geothermal gradient

f. thermal conductivity of the earth

g. time of circulation

h. depth

3. Energy generation within the system must be allowed for.

4. The allowance for a number of casing strings and a string of drill collars is unnecessary, and a wellbore of uniform hydraulic radius is adequate.

5. The assumption of steady state wellbore heat transfer is unwarranted.

6.1 Suggestions for Further Research

Variations in the drilling fluid density and heat capacity have a significant effect on the wellbore temperature distribution. However, one of the assumptions made in this study is that the fluid properties remain constant, thus simplifying the partial differential equations describing the wellbore heat transfer. If in fact, these two parameters are not temperature invariant, then the temperature distribution will be affected, and errors will occur.

It is therefore recommended that the temperature-dependent behaviour of these two parameters be investigated to ascertain whether the increased accuracy of allowing for this behaviour justifies the increased intricacy of the partial differential equations and their subsequent solution.

It is also essential that a means be available at the wellsite to accurately measure the drilling fluid heat capacity. This would constitute part of the standard procedure for measuring the fluid properties. An investigation into some simple method of obtaining this information would be of value.

There are no means available to measure the annulus temperature profile nor the dynamic bottomhole temperature, so no means exist for determining how precisely this, or previous models, predict actual temperatures in the field. The only temperatures that can be measured in the field are the inlet and outlet fluid temperatures. However, in view of the fact that the model will estimate the annulus surface temperatures, some idea of its accuracy could be obtained by comparing the measured annulus outlet temperatures with those obtained from the model.

The model also allows for the estimation of temperatures during periods of no flow, so the bottomhole temperature in the wellbore after a period of circulation, which may be obtained from a logging tool, should be estimated by the model. The comparison between these values will provide further information on the accuracy of the model.

REFERENCES

Bird, R. B. (1959), "Zur Theorie des Wärmeubergangs an nicht-Newtonische Flüssigkeiten bei laminarer Rohrströmung", Chemie Ingenieur Technik, 31, 569-572

Bogue, D. C. (1960), "Velocity Profiles in Turbulent Non-Newtonian Pipe Flow", Ph.D. Thesis, University of Delaware, Newark, Delaware

Bowen R. L. (1961), "Non-Newtonian Fluid Flow", Chem. Eng., 68, 143-150

Caldwell, D. H. and Babbitt, H. E. (1941), "Flow of Mud, Sludges and Suspensions in Circular Pipe", Ind. Eng. Chem., 33, 249-256

Cardwell, W. T. (1953), "Pressure Changes in Drilling Wells Caused by Up and Down Pipe Movement", Oil and Gas J., 52, 274-278

Chen, N. H. (1961), "Empirical Equation for Non-Newtonian Systems", Chem. Eng., 68, 152-154

Clapp, R. M. (1961), "Turbulent Heat Transfer in Pseudoplastic Non-Newtonian Fluids", International Developements in Heat Transfer, ASME, PT III, Sec A, 652-661

Charm, S. E. and Merrill, E. W. (1959), "Heat Transfer Coefficients in Straight Tubes for Pseudoplastic Food Materials in Streamline Flow", Food Res., 24, 319-331

Dodge, D. W. and Metzner, A. B. (1959), "Turbulent Flow of Non-Newtonian Systems", Amer. Inst. Chem. Eng. J., 5, 189-204

Edwardson, M. J., Girner, H. M., Parkinson, H. R., Williams, C. D. and Matthews, C. S. (1962), "Calculation of Formation Temperature Disturbances Caused by Mud Circulation", J. Pet. Tech., 14, 416-426

Farris, R. F. (1941), "A Practical Evaluation of Cements for Oil Wells", Drill. Prod. Prac., API, 283-292

Fredrickson, A. G. and Bird, R. B. (1958), "Non-Newtonian Flow in Annuli", Ind. Eng. Chem., 50, 347-352

Grigull, U. (1956), "Wärmeubergang an nicht-Newtonische Flüssigkeiten bei laminarer Rohrströmung", Chemie Ingenieur Technik, 28, 553-556

Hanks, R. W. (1963), "The Laminar-Turbulent Transition for Flow in Pipes, Concentric Annuli and Parallel Plates", Amer. Inst. Chem. Eng. J., 9, 45-48

Hanks, R.W. and Christiansen, E. B. (1962), "The Laminar-Turbulent Transition in Nonisothermal Flow of Pseudoplastic Flow in Tubes", Amer. Inst. Chem. Eng. J., 8, 467-471

Hanks, R. W. and Pratt, D. R. (1967), "On the Flow of Bingham Plastic Slurries in Pipes and Between Parallel Plates", Soc. Pet. Eng. J., 7, 342-346

Hanks, R. W. and Ricks, B. L. (1975), "Transitional and Turbulent Pipeflow of Pseudoplastic Fluids", J. Hydronautics, 9, 39-43

Holmes, C. S. and Swift, S. C. (1970), "Calculations of Circulating Mud Temperatures", J. Pet. Tech., 22, 670-674

Keller, H. H., Couch, E. J. and Berry, P. M. (1973), "Temperature Distribution in Circulating Mud Columns", Soc. Pet. Eng. J., 13, 23-30

Lakshminarayanan, M. S., Lalchandani, R. and Raja Rao, M. (1976), "Turbulent Flow Heat Transfer in Circular Tubes", Indian J. Tech., 14, 521-525

Metzner, A. B. (1965), "Non-Newtonian Heat Transfer", Advances in Heat Transfer, 2, 384-397

Metzner, A. B. and Friend, P. S. (1959), "Heat Transfer to Turbulent Non-Newtonian Fluids", Ind. Eng. Chem., 51, 879-882

Metzner, A. B. and Reed, J. C. (1955), "Flow of Non-Newtonian Fluids - Correlation of the Laminar, Transition and Turbulent Flow Regimes", Amer. Inst. Chem. Eng. J., 1, 434-440

Mishra, P. and Mishra, I. (1976), "Flow Behaviour of Power Law Fluids in an Annulus", Amer. Inst. Chem. Eng. J., 22, 617-619

Mizushina, T. and Kuriwaki, Y. (1968), "Heat Transfer to Laminar Flow of Pseudoplastic Liquids", Mem. Fac. Eng. Kyoto Univ., 30, 511-524

Mohammed, A. I. Y., Gunaji, N. N. and Smith, P. R. (1975), "Turbulent Flow of Power Law Fluids", ASCE Proc., J. Hydraulics, 101, 885-900

van Olphen, J. (1950), "Pumpability, Rheological Properties and Viscometry of Drilling Fluids", Inst. Pet. J., 36, 223-227

Oster, C. A. (1976), "Well-Hole Temperature Distribution in the Presence of Aquifers", Research Paper BNWL-SA-5658, Batelle Pacific Northwest Labs., Richland, Wash.

Peaceman, D. W. (1973), Fundamentals of Numerical Reservoir Simulation, Elsevier, Amsterdam

Raymond, L. R. (1969), "Temperature Distribution in a Circulating Drilling Fluid", J. Pet. Tech., 21, 333-341

Robertson, R. E. and Stiff, H. A. (1976), "An Improved Mathematical Model for Relating Shear Stress to Shear Rate in Drilling Fluids and Cement Slurries", Soc. Pet. Eng. J., 16, 31-36

Ryan, N. W. and Johnson, M. M. (1959), "Transition from Laminar to Turbulent Flow in Pipes", Amer. Inst. Chem. Eng. J., 5, 433-435

Savins, J. G. (1958), "Generalized Newtonian (Pseudoplastic) Flow in Stationary Pipes and Annuli", Trans. AIME, 213, 325-332

Schuh, F. J. (1964), "Computer Makes Surge Pressure Calculations Useful", Oil and Gas J., 62, 31, 96-100

Skelland, A. H. P. (1967), Non-Newtonian Flow and Heat Transfer, John Wiley & Sons Inc., New York, N.Y.

Slawomirski, M. R. (1975), "Rheological Behaviour of Oil Well Drilling Fluids", Int. J. Rock Mech. Min. Sci. Geomech. Abstr., 12, 115-123

Sullivan, W. N. (1970), "Wellbore Thermal Model", Research Paper, SAND-75-0491, Sandia Labs., Albuquerque, N.M.

Sump. G. D. and Williams, B. B. (1973), "Prediction of Wellbore Temperature During Mud Circulation and Cementing Operations", Trans. ASME, J. Eng. Ind., 95, 1083-1092

Tanaka, M. and Mitsuishi, N. (1975), "Non-Newtonian Laminar Heat Transfer in Concentric Annuli", Heat Transfer Jap. Res., 4, 2, 26-36

Tomita Y. (1961), "Analytical Treatments of Non-Newtonian Fluid Flow by Introducing the Conception of Boundary Layer", Bull. Jap. Soc. Mech. Eng., 4, 77-86

Torrance, B. McK. (1963), "Friction Factors for Turbulent Non-Newtonian Fluid Flow in Circular Pipes", South African Mech. Eng., 13, 89-91

Tragesser, A. F., Crawford, P. B. and Crawford, H. R. (1967), "A Method for Calculating Circulating Temperatures", J. Pet. Tech., 21, 1507-1512

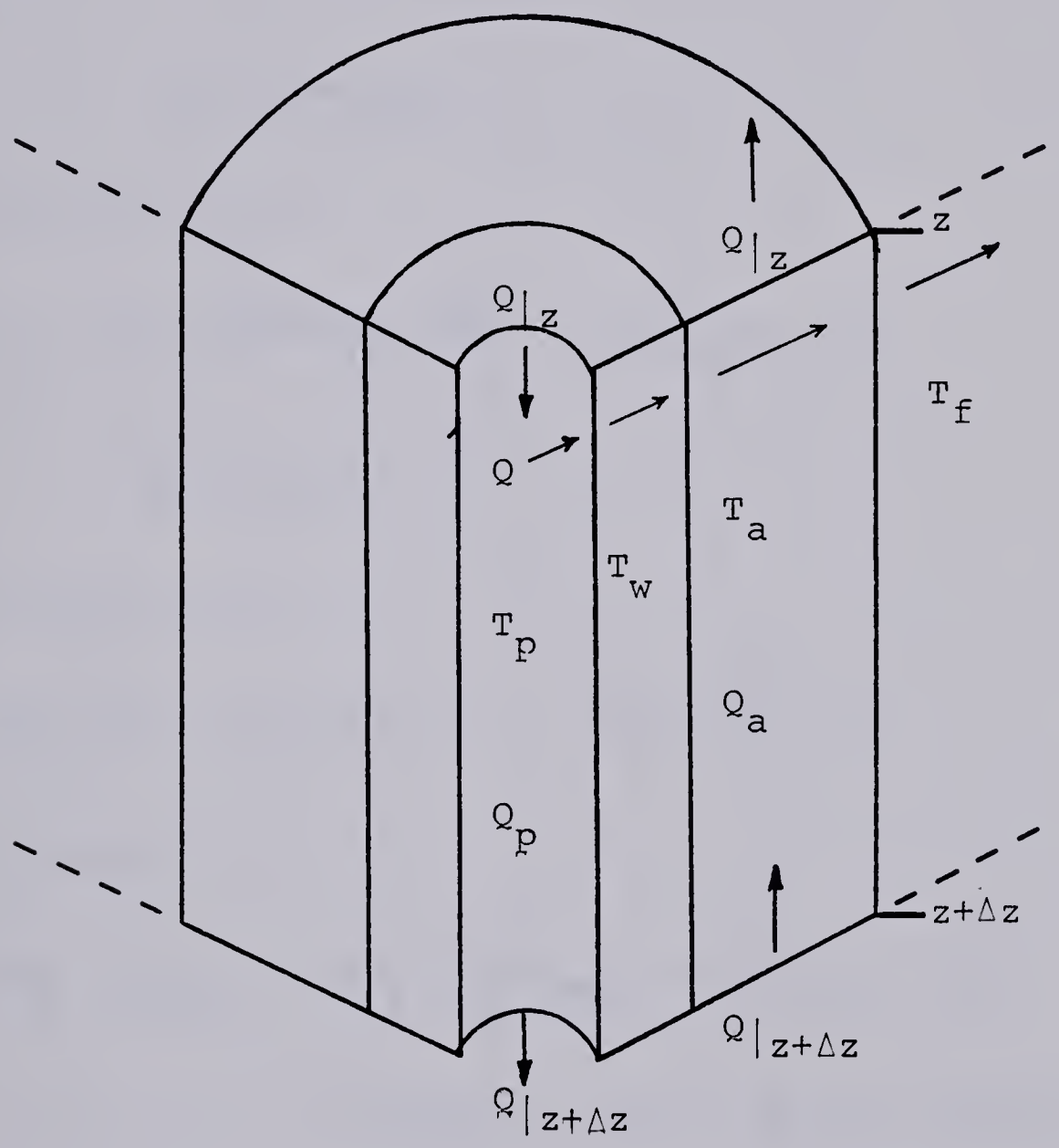
Wallick, G. C. and Savins, J. G. (1969), "A Comparison of the Differential and Integral Descriptions of the Annular Flow of a Power Law Fluid", Soc. Pet. Eng. J., 9, 311-315

Zamora, M. and Bleier, R. (1977), "The Prediction of Drilling Mud Rheology Using a Simplified Herschel-Bulkley Model", J. Press. Ves. Tech., 99, 485-490

APPENDIX I

DERIVATION OF THE PARTIAL DIFFERENTIAL EQUATIONS DESCRIBING THE TRANSIENT HEAT FLOW IN A WELLBORE

The differential element used to derive the partial differential equations describing the transient heat flow in a wellbore is depicted below.



The energy balance on the incremental volume may be expressed as follows -

Input + Generation = Output + Accumulation

FLUID IN THE DRILL PIPE:

$$\rho q C_p T_p\big|_z + Q_p\, z = \rho q C_p T_p\big|_{z+\Delta z} + 2\pi r_p h_p (T_p - T_W)\Delta z + \frac{\partial}{\partial t}(\pi r_p^2 \rho C_p T_p \Delta z) \quad \text{(A.1.1)}$$

$$Q_p \Delta z = \rho q C_p (T_p\big|_{z+\Delta z} - T_p\big|_z) + 2\pi r_p h_p (T_p - T_w)\Delta z + \frac{\partial}{\partial t}(\pi r_p^2 \rho C_p T_p \Delta z) \quad \text{(A.1.2)}$$

Dividing through by Δz

$$Q_p = \rho q C_p \frac{(T_p\big|_{z+\Delta z} - T_p\big|_z)}{\Delta z} + 2\pi r_p h_p (T_p - T_w) + \frac{\partial}{\partial t}(\pi r_p^2 \rho C_p T_p) \quad \text{(A.1.3)}$$

Taking limits as $\Delta z \to 0$

$$\rho q C_p \frac{\partial T_p}{\partial z} + 2\pi r_p h_p (T_p - T_w) = -\rho C_p \pi r_p^2 \frac{\partial T_p}{\partial t} + Q_p \quad \text{(A.1.4)}$$

DRILL PIPE WALL:

$$\pi(r_a^2 - r_p^2) q\big|_z = \pi(r_a^2 - r_p^2) q\big|_{z+\Delta z} + 2\pi r_a h_a (T_a - T_w)\Delta z + 2\pi r_p h_p (T_p - T_w)\Delta z + \frac{\partial}{\partial t}[\pi(r_a^2 - r_p^2)\rho_w C_{pw} T_w \Delta z] \quad \text{(A.1.5)}$$

Rearranging

$$0 = (r_a^2 - r_p^2) q\big|_{z+\Delta z} - (r_a^2 - r_p^2) q\big|_z + 2 r_a h_a (T_a - T_w)\Delta z + 2 r_p h_p (T_p - T_w)\Delta z + \frac{\partial}{\partial t}[(r_a^2 - r_p^2)\rho_w C_{pw} T_w \Delta z] \quad \text{(A.1.6)}$$

Dividing through by Δz and taking limits as $\Delta z \to 0$

$$0 = \frac{\partial}{\partial z}\left[(r_a^2 - r_p^2)q\Big|_z\right] + 2r_a h_a(T_a - T_w) + 2r_p h_p(T_p - T_a)$$

$$+ (r_a^2 - r_p^2)\rho_w C_{pw}\frac{\partial T_w}{\partial t} \qquad \text{(A.1.7)}$$

But from Fourier's Law, $q_z = -k_w \frac{\partial T_w}{\partial z}$

$$k_w \frac{\partial^2 T_w}{\partial z^2} + \frac{2r_p h_p}{(r_a^2 - r_p^2)}(T_p - T_w) + \frac{2r_a h_a(T_a - T_w)}{(r_a^2 - r_p^2)} = \rho_w C_{pw}\frac{\partial T_w}{\partial t} \qquad \text{(A.1.8)}$$

FLUID IN THE ANNULUS:

$$\rho q C_p T_a\Big|_{z+\Delta z} + Q_a \Delta z = \rho q C_p T_a\Big|_z + 2\pi r_a h_a(T_a - T_w)\Delta z$$

$$+ 2\pi r_o h_o(T_a - T_f)\Delta z$$

$$+ \frac{\partial}{\partial t}\left[\pi(r_o^2 - r_a^2)\rho C_p T_a \Delta z\right] \qquad \text{(A.1.9)}$$

Rearranging

$$Q_a \Delta z = -\rho q C_p(T_a\Big|_{z+\Delta z} - T_a\Big|_z) + 2\pi r_a h_a(T_a - T_w)\Delta z$$

$$+ 2\pi r_o h_o(T_a - T_f)\Delta z + \frac{\partial}{\partial t}\left[\pi(r_o^2 - r_a^2)\rho C_p T_a \Delta z\right] \qquad \text{(A.1.10)}$$

Dividing through by Δz

$$Q_a = -\rho q C_p \frac{(T_a\Big|_{z+\Delta z} - T_a\Big|_z)}{\Delta z} + 2\pi r_a h_a(T_a - T_w)$$

$$+ 2\pi r_o h_o(T_a - T_f) + \frac{\partial}{\partial t}\left[\pi(r_o^2 - r_a^2)\rho C_p T_a\right] \qquad \text{(A.1.11)}$$

Taking limits as $\Delta z \to 0$

$$\rho q C_p \frac{\partial T_a}{\partial z} + 2\pi r_a h_a (T_w - T_a) + 2\pi r_o h_o (T_f - T_a) = \rho C_p \pi (r_o^2 - r_a^2) \frac{\partial T_a}{\partial t} \qquad \text{(A.1.12)}$$

FORMATION:

The general energy equation for a two-dimensional system, neglecting the radial temperature gradient and viscous dissipation, may be written as -

$$\rho_f C_{pf} \frac{\partial T_f}{\partial t} + V_z \frac{\partial T_f}{\partial z} = \frac{k_f}{r} \frac{\partial}{\partial r} \left(r \frac{\partial T_f}{\partial r} \right) + \frac{\partial^2 T_f}{\partial z^2} \qquad \text{(A.1.13)}$$

$V_z = 0$ in the formation

Therefore

$$\frac{\partial^2 T_f}{\partial z^2} + \frac{\partial^2 T_f}{\partial r^2} + \frac{1}{r} \frac{\partial T_f}{\partial r} = \frac{\rho_f C_{pf}}{k_f} \frac{\partial T_f}{\partial t} \qquad \text{(A.1.14)}$$

APPENDIX II

DERIVATION OF THE FINITE DIFFERENCE EQUATIONS

Writing the partial differential equations derived in Appendix I in finite difference form involves representing the first order derivatives by two-point forward and backward difference approximations, and the second order derivatives by three-point centred difference approximations.

The four partial differential equations can be written in implicit finite difference form for each vertical element j of thickness Δz_j, and for a time step of Δt as follows -

FLUID IN THE DRILL PIPE:

$$\rho q C_p \frac{\left(T^{n+1}_{1,j-1} - T^{n+1}_{1,j}\right)}{\Delta z_j} + 2\pi r_p h_p \left(T^{n+1}_{2,j} - T^{n+1}_{1,j}\right)$$

$$= - \pi r_p \rho C_p \frac{\left(T^{n+1}_{1,j} - T^{n}_{1,j}\right)}{\Delta t} + Q_p \qquad \text{(A.2.1)}$$

DRILL PIPE WALL:

$$\frac{k_w}{\Delta z_j}\left[\frac{\left(T^{n+1}_{2,j+1} - T^{n+1}_{2,j}\right)}{\Delta z_{j+0.5}} - \frac{\left(T_{2,j} - T_{2,j-1}\right)}{\Delta z_{j-0.5}}\right]$$

$$+ \frac{2r_p h_p}{(r_a^2 - r_p^2)}\left(T^{n+1}_{1,j} - T^{n+1}_{2,j}\right) - \frac{2r_a h_a}{(r_a^2 - r_p^2)}\left(T^{n+1}_{2,j} - T^{n+1}_{3,j}\right)$$

$$= \rho_w C_{pw} \frac{\left(T^{n+1}_{2,j} - T^{n}_{2,j}\right)}{\Delta t} \qquad \text{(A.2.2)}$$

FLUID IN THE ANNULUS

$$qC_p \frac{\left(T_{3,j+1}^{n+1} - T_{3,j}^{n+1}\right)}{z_j} + 2\pi r_a h_a \left(T_{2,j}^{n+1} - T_{3,j}^{n+1}\right)$$

$$+ 2\pi r_o h_o \left(T_{4,j}^{n+1} - T_{3,j}^{n+1}\right)$$

$$= \pi(r_o^2 - r_a^2)\rho C_p \frac{\left(T_{3,j}^{n+1} - T_{3,j}^{n}\right)}{\Delta t} - Q_a \qquad \text{(A.2.3)}$$

FORMATION:

$$\frac{\partial^2 T_f}{\partial z^2} \equiv \frac{1}{\Delta z_j}\left[\frac{\left(T_{i,j+1}^{n+1} - T_{i,j}^{n+1}\right)}{\Delta z_{j+0.5}} - \frac{\left(T_{i,j}^{n+1} - T_{i,j-1}^{n+1}\right)}{\Delta z_{j-0.5}}\right] \qquad \text{(A.2.4)}$$

$$\frac{k_f}{r}\frac{\partial}{\partial r}\left(r\frac{\partial T_f}{\partial r}\right) \equiv \frac{k_f}{r_i}\left\{\frac{1}{\Delta r}\left[r_{i-0.5}\frac{\partial}{\partial r}(T_{i-0.5}) - r_{i+0.5}\frac{\partial}{\partial r}(T_{i+0.5})\right]\right\} \qquad \text{(A.2.5)}$$

$$\frac{\partial}{\partial r}(T_{i-0.5}) = \frac{1}{\Delta r}(T_{i-1} - T_i) \qquad \text{(A.2.6)}$$

$$\frac{\partial}{\partial r}(T_{i+0.5}) = \frac{1}{\Delta r}(T_i - T_{i+1}) \qquad \text{(A.2.7)}$$

From Fourier's Law

$$q = 2\pi r k_f \frac{dT_f}{dL} = 2\pi r_{i+0.5} k_f \frac{(T_{i+1} - T_i)}{(r_{i+1} - r_i)} \qquad \text{(A.2.8)}$$

For radial heat flow

$$q = \frac{2\,k_f(T_1 - T_2)}{\ln(r_2/r_1)} = \frac{2\,k_f(T_{i+1} - T_i)}{\ln\left(\frac{r_{i+1}}{r_i}\right)} \qquad \text{(A.2.9)}$$

Equating Equations A.2.8 and A.2.9

$$r_{i+0.5} = \frac{r_{i+1} - r_i}{\ln\left(\frac{r_{i+1}}{r_i}\right)} \qquad \text{(A.2.10)}$$

$$r_{i-0.5} = \frac{r_i - r_{i-1}}{\ln\left(\frac{r_i}{r_{i-1}}\right)} \qquad \text{(A.2.11)}$$

Substituting into Equation A.2.5

$$\frac{k_f}{r}\,\frac{\partial}{\partial r}\left(r\,\frac{\partial T_f}{\partial r}\right) = \frac{k_f}{r_i \Delta r}\left[\frac{1}{\ln\left(\frac{r_i}{r_{i-1}}\right)}(T_{i-1} - T_i) - \frac{1}{\ln\left(\frac{r_{i+1}}{r_i}\right)}(T_i - T_{i+1})\right] \qquad \text{(A.2.12)}$$

Therefore

$$\frac{1}{\Delta z_j}\left[\frac{\left(T_{i,j+1}^{n+1} - T_{i,j}^{n+1}\right)}{\Delta z_{j+0.5}} - \frac{\left(T_{i,j}^{n+1} - T_{i,j-1}^{n+1}\right)}{\Delta z_{j-0.5}}\right]$$

$$+ \frac{1}{r_i \Delta r}\left[\frac{1}{\ln\left(\frac{r_i}{r_{i-1}}\right)}\left(T_{i-1,j} - T_{i,j}\right) - \frac{1}{\ln\left(\frac{r_{i+1}}{r_i}\right)}\left(T_{i,j} - T_{i+1,j}\right)\right]$$

$$= \frac{\rho_f C_{p_f}}{k_f}\,\frac{\left(T_{i,j}^{n+1} - T_{i,j}^{n}\right)}{\Delta t} \qquad \text{(A.2.13)}$$

where

$r_i = 2r_o + (2i - 7)\Delta r$

Δr = Width of each of the external radial elements

$5 \leq i \leq 10$

APPENDIX III

SUBROUTINE LEQT1B

The linear system of equations describing the transient heat flow in the wellbore is expressed in matrix form in Equation A.3.1

$$[A].\{T\} = \{C\} \qquad (A.3.1)$$

where A is the coefficient matrix in band storage form, T is the unknown temperature vector at the new time level and C is the vector containing the right hand sides of the equations.

Solution of this equation to obtain the values of the T vector is achieved by means of the International Mathematics and Statistics Library (IMSL) subroutine LEQT1B. This subroutine solves the general equation A.3.2 by first factorizing the coefficient matrix into lower and upper triangular matrices.

$$[A].[X] = [B] \qquad (A.3.2)$$

It then solves for each element of the unknown matrix X by backward substitution.

In the specific case being considered here, the matrices X and B are replaced by vectors T and C, respectively.

The sample output included in Appendix IV was obtained from the data of Table 4-1. Once the computer program had calculated the coefficients in matrix A and the right hand terms contained in vector C, LEQT1B was used to solve Equation A.3.2 for T.

The parameter list of subroutine LEQT1B, with a brief definition of each of the parameters and the corresponding

value of the parameter for this particular example, are given below.

Parameter	Definition	Value
A	Coefficient matrix	
N	Order of matrix A	1560
NLC	Number of lower codiagonals	12
NUC	Number of upper codiagonals	10
IA	Number of rows in A	1560
B	Right hand side matrix	
M	Number of columns in B	1
IB	Number of rows in B	1560
IJOB	Operation flag (see below)	0
XL	Work area of minimum size N x (NLC + 1)	21000
IER	Error parameter in output	

The mesh-centred grid representing the 15,000 feet wellbore is composed of 156 vertical elements and 10 radial elements. After the steps outlined in Chapter 3 have been carried out, this is transformed into a 1560 x 21 band storage matrix. The addition of the two extra columns to allow for the equalization of temperatures at the drill bit increases the band storage matrix to 1560 x 23 elements. Thus, the coefficient matrix A, in band storage form, comprises 1560 rows, 12 columns to the left of the main diagonal and 10 columns to the right of the main diagonal.

When the operation flag IJOB is zero, the complete

solution procedure is carried out with the solution matrix replacing the right hand side matrix on output. In this case, the solution vector T replaces the right hand side vector C which then contains the new temperatures.

If IJOB = 1, only the factorization occurs and if IJOB = 2, only the backward substitution takes place. Hence, IJOB = 2 presupposes that LEQT1B has already been called with IJOB = 1 or 0.

B30270